Advances in Engineering Software 100 (2016) 82–96

Contents lists available at ScienceDirect

Advances in Engineering Software

journal homepage: www.elsevier.com/locate/advengsoft

Research Paper

Modification of the Audze–Eglājs criterion to achieve a uniform distribution of sampling points

Jan Eliáš*, Miroslav Vořechovský

Institute of Structural Mechanics, Faculty of Civil Engineering, Brno University of Technology, Czech Republic

ARTICLE INFO

Article history:
Received 2 December 2015
Revised 14 June 2016
Accepted 13 July 2016

Keywords:
Design of experiments
Periodic boundary conditions
Latin Hypercube sampling
Uniform distribution
Combinatorial optimization
Audze–Eglājs criterion
Audze-Eglais criterion

ABSTRACT

The Audze–Eglājs (AE) criterion was developed to achieve a uniform distribution of experimental points in a hypercube. However, the paper shows that the AE criterion provides strongly nonuniform designs due to the effect of the boundaries of the hypercube. We propose a simple remedy that lies in the assumption of periodic boundary conditions. The biased behavior of the original AE criterion and excellent performance of the modified criterion are demonstrated using simple numerical examples focused on (i) the uniformity of sampling density over the design space and, (ii) statistical sampling efficiency measured through the ability to correctly estimate the statistical parameters of functions of random variables. An engineering example of reliability calculation is presented, too.

1. Introduction

This article considers the choice of an experimental design for computer experiments. The choice of experimental points is an important issue in planning an efficient computer experiment. The methods used for formulating the plan of experimental points are collectively known as Design of Experiments (DoE). DoE is a crucial process in many engineering tasks. Its purpose is to provide a set of N_{sim} points (a sample) lying inside a chosen *design domain* that are optimally distributed; the optimality of the experimental points depends on the nature of the problem. Various authors have suggested intuitive goals for good designs, including “good coverage”, the ability to fit complex models, many levels for each factor, and good projection properties. At the same time, a number of different mathematical criteria have been put forth for comparing designs.

There are two main application areas for DoE methods in the area of computer experiments. First, DoE is often used for evaluating the effects of different parameters of a function while searching for a response surface. The choice of location for the evaluation points or plan points is important in order to obtain a good approximation of the response surface. A surrogate model that approximates the original, complex, model, can be e.g. a response surface [32], a support vector regression or a neural network [25]. The surrogate model is based on a set of carefully selected points in the domain of variables. The process of finding optimal experimental points might be performed adaptively, i.e. in several sequential steps, where the location of the additional points in every step are based on result achieved so far [49].

Second, the selection of the sampling points is even more important when evaluating approximations to integrals as is performed in Monte Carlo simulations (numerical integration), where equal sampling probabilities inside the design domain are required. These integrals may, for example, represent variables being estimated in uncertainty analyses. The evaluation of the uncertainty associated with analysis outcomes is now widely recognized as an important part of any modeling effort. A number of approaches to such evaluation are in use, including neural networks [6], variance decomposition procedures [27,42], and Monte Carlo (i.e. sampling-based) procedures [16,46].

In both applications mentioned above, it is convenient when the probability that the ith experimental point is located inside some chosen subset of the domain equals to V_S/V_D, with V_S being the subset volume and V_D the volume of the whole domain (for unconstrained design $V_D = 1$). Whenever this is valid, the design criterion will be called *uniform*. Even though such uniformity is conceptually simple and intuitive on a qualitative level, it is somewhat complicated to describe and characterize it mathematically. Although some problems do not require this uniformity, it is the crucial assumption in Monte-Carlo integration and its violation may (as will be demonstrated below) lead to significant errors.

* Corresponding author. Tel.: +420541147132.
E-mail address: elias.j@fce.vutbr.cz (J. Eliáš).

http://dx.doi.org/10.1016/j.advengsoft.2016.07.004
0965-9978/

The process of finding the experimental points can be understood as an optimization problem: we are searching for a design that minimizes an objective function, E. After an initial set of experimental points have been generated (typically via a pseudo-random generator), some modifications of them are performed in sequential steps to find the minimum of the objective function. Several optimization algorithms can be utilized; simulated annealing [57] will be employed in this paper. The chosen optimization algorithms may strongly affect the number of optimization steps and therefore the time to achieve the minimum, as well as the ability to find the global minimum among many extremes (local minima). However, the quality of the design is controlled by a chosen objective function (or design criterion).

Several criteria (objective functions) have been developed and used [21], e.g. the Audze-Eglājs (AE) criterion [1], the Euclidean MaxiMin and MiniMax distance between points [22], Modified L2 discrepancy [8], Wrap-Around L_2-Discrepancy [7], Centered L_2-discrepancy [9], the $D-$optimality criterion [50], criteria based on correlation (orthogonality) [54,55,57], Voronoi tessellation [45], the ϕ criterion introduced in [31], dynamic modeling of an expanding lattice, designs maximizing entropy [48], integrated mean-squared error [47], and many others. Some authors believe that in order to obtain a versatile (robust) design, several criteria should be used simultaneously [13].

It should be also noted that an experimental design can be also obtained via so-called "quasi-random" low-discrepancy sequences (deterministic versions of MC analysis) that can often achieve reasonably uniform point placement in hypercubes. One such example is the Niederreiter sequence [37]. Actually, fairly uniform point distributions can be produced by Halton [15] and Sobol' [51] sequences despite the flexibility of sample size selection: the points are added one-at-a-time to the design space. For resolving response probabilities, the Hammersley and modified-Halton methods were found in [44] using several test problems to perform only slightly better than Latin Hypercube Sampling. However, when the hyperspace dimension N_{var} becomes moderate to large and/or N_{sim} becomes high, usually these sequences suffer from spurious sample correlation [10,19]. These deterministic techniques are not further exploited in the paper.

Several authors have proposed a combination of uniformity criteria with Latin Hypercube Sampling (LHS) [5,20,30] as a representative of variance reduction techniques (these designs are sometimes named optimal LHS). Tang [53] has introduced orthogonal-array-based Latin hypercubes to improve projections on higher dimensional subspaces, the space-filling properties of which were *supposedly* improved in [26] by using the Audze-Eglājs criterion (without explicitly citing [1]). LHS is a type of stratified sampling technique; the coordinates of N_{sim} experimental points (simulations) are sampled from N_{sim} equidistant subintervals of length $1/N_{\text{sim}}$ so that every subinterval contains one and only one point. LHS guarantees the uniform distribution of experimental points along each dimension where it is used, typically along all N_{var} dimensions. The frequently used version of LHS limits the selection of coordinates along each variable to fixed set of values, most often the centers of the intervals (called LHS-median in [57]) with coordinates $(i-0.5)/N_{\text{sim}}$ for $i \in \langle 1, 2, \ldots, N_{\text{sim}} \rangle$. Such a type of LHS will be used in this paper. When optimizing an existing LH sample, discrete domain consisting of interval centers is prescribed for each variable, so the remaining task is to perform pairing (changing mutual orderings = shuffling) in order to minimize the DoE criterion.

The design of experiments is typically performed in a hypercubical domain of N_{var} dimensions, where each dimension/variable, U_v, ranges between zero and one ($v = 1, \ldots, N_{\text{var}}$). Sometimes, additional constraints are required and the design of experiments is performed in a constrained domain and becomes more complicated [33,41]. In this paper, the *design domain* is a classical N_{var}-dimensional unit hypercube. This *design domain* is to be covered by N_{sim} points as evenly as possible.

This paper is focused on the performance of the widely used Audze-Eglājs (AE) criterion and its improvement. It is shown that the original AE criterion provides designs that are not *uniform*. The appendix provides a simple explanation for this bias that arises from the presence of hypercube boundaries. Therefore, a remedy leading to uniform designs that involve the assumption of periodicity is introduced. The remedy does not increase computational complexity and is extremely easy to implement in source codes that already contain an evaluation of the original AE criterion. Three simple numerical examples are performed to show that (i) the sampling bias in the original AE criterion leads to errors in the estimation of moments of statistical models and (ii) the improved periodic criterion provides correct values with low variance. Finally, a finite element model with a nonlinear constitutive law for concrete beam loaded in bending, featuring four random variables, shows the bias in calculation of probability of failure when the original AE criterion is used.

2. Review of the original AE criterion

The AE criterion was developed by Audze and Eglājs [1]. The authors claimed that the criterion may be understood to express the potential energy of a system of particles with repulsive forces between each pair of them; minimization of this potential energy optimizes the spatial arrangement of the points. The repulsive forces between pairs of points are functions of their distance. The Euclidean distance, L_{ij}, between points (realizations) $\boldsymbol{u}_i = \left(u_{i,1}, u_{i,2}, \ldots, u_{i,N_{\text{var}}}\right)$ and $\boldsymbol{u}_j$ in N_{var}-dimensional space can be expressed as a function of their coordinates

$$L_{ij} = L\left(\boldsymbol{u}_i, \boldsymbol{u}_j\right) = \sqrt{\sum_{v=1}^{N_{\text{var}}} \left(u_{i,v} - u_{j,v}\right)^2} = \sqrt{\sum_{v=1}^{N_{\text{var}}} \left(\Delta_{ij,v}\right)^2} \tag{1}$$

where

$$\Delta_{ij,v} = |u_{i,v} - u_{j,v}| \tag{2}$$

is the distance between two points measured along (or projected onto) axis/dimension v (difference in variable U_v); $|X|$ stands for the absolute value of X. Each variable U_v ranges between zero and one, therefore $\Delta_{ij,\,v}$ has the same limits: $\Delta_{ij,\,v} \in \langle 0, 1 \rangle$. The Audze-Eglājs criterion is defined using the squared Euclidean distances between all pairs of experimental points as

$$E^{\text{AE}} = \sum_{i=1}^{N_{\text{sim}}} \sum_{j=i+1}^{N_{\text{sim}}} \frac{1}{L_{ij}^2} \tag{3}$$

Several authors claim that the force interactions mimic gravitational forces. For example, Bates et al. [3] claim that "if the magnitude of the repulsive forces is inversely proportional to the distance squared between the points" then Eq. (3) represents potential energy. Similar statements are to be found in [11,18,58,59]. In [24], the authors, in contrast, claim that the AE criterion "is equal to the minimum of potential energy of repulsive forces for the points with unity mass if the magnitude of these repulsive forces is inversely proportional to the distance between the points". We disagree with both these explanations. If the criterion quantifies the potential energy of a system of particles, the repulsive force between pairs of particles must be equal to the negative derivative of the contact potential energy with respect to distance

$$F_{ij} = -\frac{\mathrm{d}\, E_{ij}^{\text{AE}}}{\mathrm{d}\, L_{ij}} = -\frac{\mathrm{d}\, \frac{1}{L_{ij}^2}}{\mathrm{d}\, L_{ij}} = \frac{2}{L_{ij}^3} \tag{4}$$

Therefore, the AE criterion assumes that the repulsive forces between particles are inversely proportional to the distance between them raised to the *third power*. One can develop similar criteria based on another force-distance relation, e.g. with $F_{i,j} = 1/(L_{ij})^2$, which would result in the potential energy (and corresponding design criterion) $1/L_{ij}$.

Note that with increasing power in the criterion Eq. (3), the contribution of short distances tends to be increasingly emhasized. The limit of the criterion in Eq. (3) as the power approaches infinity corresponds to a simple dependence on the shortest distance (the distance between the closest pair of points). This can be shown by calculating the limit of the pth root of the E^{AE} with increased power p using the following equality: $\lim_{p\to\infty} \sqrt[p]{\sum_i X_i^p} = \max X_i$

$$\lim_{p\to\infty} \sqrt[p]{\sum_{i\neq j} \frac{1}{L_{ij}^p}} = \max_{i\neq j} \frac{1}{L_{ij}} = \frac{1}{\min_{i\neq j} L_{ij}} \tag{5}$$

To minimize the energy with increased power (which corresponds to minimization of the pth root of it), one would need, at the limit, to maximize the minimum over the distances in the design domain, i.e. the MaxiMin criterion would be recovered. Note that the ϕ criterion proposed by Morris and Mitchell (see Eq. (2.1) in [31]) is a generalization of the AE criterion with a fixed p as a positive integer, as used in our Eq. (5).

2.1. Selected existing applications of AE criterion

The AE criterion has been utilized by many authors. The authors of [43] identified the elastic properties of composites by exploiting a response surface built using points obtained by DoE optimized with the AE criterion. The AE criterion has been proposed as one of the criteria to be used for the optimization of experimental designs for metamodeling [2]. The AE criterion has also been used for planning the experimental design for the identification of the elastic properties of composite plate [24]. The original AE criterion has been used as one of the criteria employed in the optimization of the sample size extension of an existing LH sample [56] and implemented in FReET software [38].

One of the possible applications of the AE criterion is in the optimization of samples used in Monte Carlo numerical integration, e.g. statistical analyses of functions involving random variables. AE criterion can be used when optimizing samples obtained by crude Monte Carlo Sampling (independent sampling on the $\langle 0,1\rangle$ interval). It is well recognized that such a crude Monte Carlo Sampling does not perform well when it comes to uniformly spreading out the experimental points with respect to the target density function. This is a pronounced issue especially for small sample sizes. An improvement in reducing the variance of estimated statistics can be achieved by LHS. The AE criterion can then be employed in combination with the LHS strategy, the concept for which appeared in Bates et al. [3] and Husslage et al. [18]. Later, Fuerle and Sienz [11] used the LHS-AE combination for sampling from constrained design spaces (unit hypercubes reduced in size via the removal of infeasible regions). This method has been applied to the problem of optimizing carbon-fiber bicycle frames [12]. Further, Latin Hypercube design with the ordering of point coordinates optimized using the AE criterion was suggested in [3], and its computer implementation named M-Explore (an extension of Radioss software) has been published in [4]. In [28] the authors recommend optimizing LHS based on the AE criterion rather than the minimum distance criterion. LHS designs optimized using AE have been applied to a variety of problems such as the optimization of bread-baking ovens [23], structural system parameter identification using the finite element method [35], the construction of a response surface with the exploitation of proper generalized decomposition [14], and the solution a problem concerning system identification in vehicle-structure interaction [34].

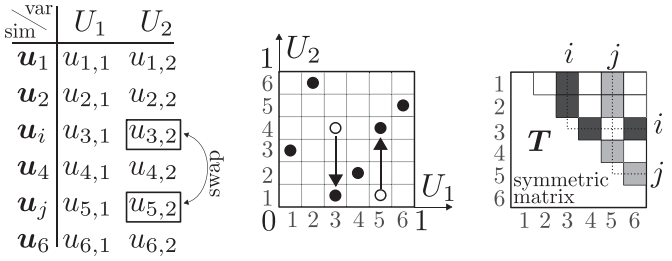

Fig. 1. Swap (exchange) of coordinates i and j of variable U_2 in the sampling plan (left); in a bivariate scatterplot (middle); affected elements in a square symmetrical matrix $\boldsymbol{T}$ of inverted squared pair distances between the points (right).

3. Optimization of a sample using the AE criterion

In sampling analyses, the preparation of a sample is, in fact, the preparation of a sampling plan, i.e. a matrix of size $N_{\mathrm{sim}} \times N_{\mathrm{var}}$. Fig. 1 left shows a sampling plan for two variables and six simulations in the form of a table. When combining sampling strategies with given coordinates for each separate variable (as in the case of LHS), the only way to optimize the sample with respect to a particular criterion (correlation, AE criterion) is to change the mutual ordering of these coordinates. In this paper, we focus on LHS, in which each variable (dimension) has N_{sim} fixed coordinates (e.g. centers of N_{sim} equidistant intervals). To minimize E^{AE}, one can search among all $(N_{\mathrm{sim}}!)^{N_{\mathrm{var}}-1}$ possible mutual orderings of these fixed coordinates. We use simulated annealing optimization [57] to search for a good solution; however other techniques such as genetic algorithms can be effectively utilized [3,59]. It involves the subsequent swapping of the coordinates of a pair of points (see the exchange of coordinates in Fig. 1 middle). The element-exchange within a column (a variable) simply interchanges two entries selected for a given variable and therefore such an operation maintains the LHS property. However, this swap affects selected entries in the distance matrix (Fig. 1 right) and always leads to a change in the value of the optimized function (non-collapsing design due to LHS sampling). Such a swap is accepted whenever it decreases the value of the optimized function. In cases when the swap leads to an increase in the criterion, its acceptance depends on a *cooling schedule*, i.e. (i) on how much the value is worse than the one before the swap, (ii) on a generated value for a uniform random variable and, (iii) on the temperature of the system (the temperature is decreasing during the process). Details regarding this heuristic optimization algorithm can be found in [57].

Regarding implementation details and the speed of execution of the AE criteria, we should mention the fact that complete evaluation of the energy norm (Eq. (3)) is not necessary after every swap of a pair of point coordinates. For small to moderate N_{sim}, it is worthwhile to save the symmetrical matrix of inverse squared distances, $\boldsymbol{T}$: $T_{ij} = 1/L_{ij}^2$, into computer memory. The value of the AE criterion is simply the sum of the elements in the upper triangle of matrix $\boldsymbol{T}$. Each swap of two coordinates in the sampling plan necessitates update of $2 \times (N_{\mathrm{sim}} - 2)$ entries in matrix $\boldsymbol{T}$. For both swapped points, i and j, there are always $N_{\mathrm{sim}} - 2$ updated distances. The following four distances remain unchanged: L_{ii}, L_{jj}, L_{ij} and L_{ji}, see Fig 1 right. Before updating the $\boldsymbol{T}$ matrix, the modified entries can be subtracted from the norm (energy), then $\boldsymbol{T}$ gets updated and the changed terms are added to the norm. Computation of the AE criterion by summing all entries of the triangular matrix $\boldsymbol{T}$ is only needed after a certain number of swaps to avoid rounding errors.

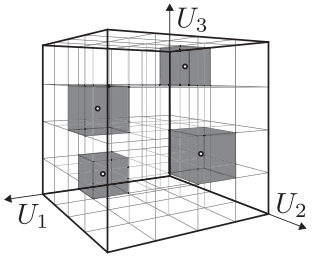

Fig. 2. The considered *design domain* – a unit hypercube ($N_{\text{var}} = 3$) divided into bins of equal volumes. Boxes with $N_{\text{sim}} = 4$ experimental points are highlighted.

4. Biased design

The *supposed uniformity* [1,3,17,18,21,24,28,58,59] of the original AE design is critically evaluated in this section. As mentioned in Introduction, the probability that the ith experimental point will be located inside some chosen subset of the domain must be equal to V_S/V_D, with V_S being the subset volume and V_D the volume of the whole domain (for unconstrained design $V_D = 1$).

Since we are using LHS, the coordinates of the points are known and the whole unit hypercube of volume $V_D = 1^{N_{\text{var}}} = 1$ can be divided into ${N_{\text{sim}}}^{N_{\text{var}}}$ bins of the same volume using the grid of equidistant coordinates along each dimension, see Fig. 2. A uniform design is achieved if the probability of filling each of these bins is identical. In order to perform a numerical test of AE-optimized LHS designs, N_{run} designs (sampling plans of dimensions $N_{\text{var}} \times N_{\text{sim}}$) have been simulated and optimized. After generating the N_{run} designs, the total number of sampled points is $N_{\text{sim}}N_{\text{run}}$. The average number of points inside one bin should be for *uniform* design $f_a = N_{\text{sim}}N_{\text{run}}/{N_{\text{sim}}}^{N_{\text{var}}} = N_{\text{run}}/{N_{\text{sim}}}^{N_{\text{var}}-1}$. For each bin, we now count the actual frequency of occurrence of the points inside that bin, f. Finally, we define a variable $\bar{f}$ (a normalized frequency) that can be calculated for each bin using the ratio

$$\bar{f} = f\frac{1}{f_a} = f\frac{{N_{\text{sim}}}^{N_{\text{var}}-1}}{N_{\text{run}}} \tag{6}$$

An ideal design criterion should produce $\bar{f} = 1$ for all of the bins.

The results of the numerical study are shown in Figs. 3 top and 4 top for various numbers of points N_{sim} and dimensions N_{var} in 2D images. The number of repetitive optimized designs used, $N_{\text{run}} = 10^7$, is high enough to reveal unwanted patterns. The shade of gray color represents the $\bar{f}$ value at individual LHS points (bins). The first dimension (variable) is associated with the horizontal axis, the second variable with the vertical axis, and the third variable (if present) is captured by repetitive 2D images (slices) produced for different values of the third coordinate. Similarly, the fourth dimension (if present) is shown by repetitive views of 3D plots made for different values of the fourth coordinate.

The figures clearly show the *non-uniformity* of point density in the design domain when the original AE criterion is used for optimization. In 2D space, the corners are not sampled at all, but there is an area of highly probable points close to them followed again by an improbable region. A similar behavior is observed in 3D and 4D spaces, where the corners of the domain are always sampled poorly. The plot for $N_{\text{var}} = 3$ shows a formation resembling a sphere with an empty interior (low N_{sim}) or with a less-accentuated second interior sphere (higher N_{sim}). For $N_{\text{var}} = 4$, a similar hypersphere forms. Generally, the tendency to avoid the corners of the hypercube is apparent. The more coordinates that reach its extremes (0 or 1) at the corner/edge, the more pronounced the effect, i.e. in 3D, corners are more "repellent" than edges.

The fact that LHS design optimized with the AE criterion does not cover corners in 2D domains was also noticed in [59], the authors of which wrote: "One of the shortcomings of LH DoEs is that it is not possible to have points at all the extremities (corner points) of the design space due to the rule of one point per level". As a remedy, the authors of [59] used fixed points in the corners of the design domain to solve the problem. Our paper shows that this explanation of the problem is wrong because the problem is in the criterion itself; the solution of fixing the corner points is not consistent with the requested properties of the design. Appendix A provides proof that the original AE criterion delivers a non-uniform distribution of points over the design space, and thus explains the source of the bias.

While Figs. 3 top and 4 top show the density of the point occupation of bins from $N_{\text{run}} = 10^7$ AE-optimized LHS designs, Fig. 5 left shows just one run - a single LH-sample set optimized in 2D and 3D domains. The irregularity of point coverage (empty corners) is accentuated by periodic repetition of the unit square in the plot. The middle column shows a regular LHS design optimized using the "PAE" criterion proposed below in this paper. The right column shows an LHS design obtained with a correlation (orthogonality) criterion [57], i.e. a criterion frequently used in practice; these LH-samples are denoted as COR designs. The main purpose of the figure is to once again demonstrate the empty corners that are not sampled when using the original AE formulation. All of the designs in Fig. 5 are LHS designs and therefore the 1D projections of points are perfectly uniform (they form a grid of equidistant points). From a visual comparison of 2D AE (and PAE) and COR designs, it is clear that the dispersion is much better for PAE. The reason is that in 2D designs, the visualized 2D lengths between points are directly subject to optimization. On the other hand, the three projections of 3D designs seem to show similar degree of clustering for both PAE and COR designs. The reason is that the AE (and PAE) criterion optimizes the 3D distances and not the 2D projections of distances. The 2D scatter-plots are not sufficient to reveal the better dispersion of PAE over COR in higher dimensions. AE and PAE criteria optimize N_{var}-dimensional lengths and LHS itself guarantees perfect 1D spacings. To get LHS designs with a uniform distribution of points in all possible projections into spaces of dimensions from 2 to $N_{\text{var}} - 1$, the criterion would have to consider all of these projections.

After the above demonstration of the undesired non-uniformity of the AE criterion, the paper continues with a description of a very simple and computationally cheap remedy that provides *uniform* designs while keeping the concept of the AE criterion (the analogy between the point distribution and minimizing the energy of a system of charged particles) unchanged.

5. The AE criterion in periodic space

The remedy proposed here, which leads to *uniform* designs, is based on periodic repetition of the unit hypercube (Fig. 2) containing experimental points along all directions/variables of the design domain; see Fig. 6 for $N_{\text{var}} = 2$. We consider periodic images of the ith point to have coordinates $u_{i,v} + k_{i,v}$ where the dimension/variable is denoted $v \in \{1, 2, \ldots, N_{\text{var}}\}$ and k is an arbitrary integer. When k equals zero for all v, we obtain the original point placed inside the design domain. The ideal would be to optimize the potential energy of such an infinite periodic system based on the original formulation of the AE criterion. One can see that the whole system of pairs of points is just an image – repeated infinitely many times – of a *basic* system containing all pairs where at least one of the points belongs to the original set of points. Therefore, it is sufficient to deal with the *basic* system only.

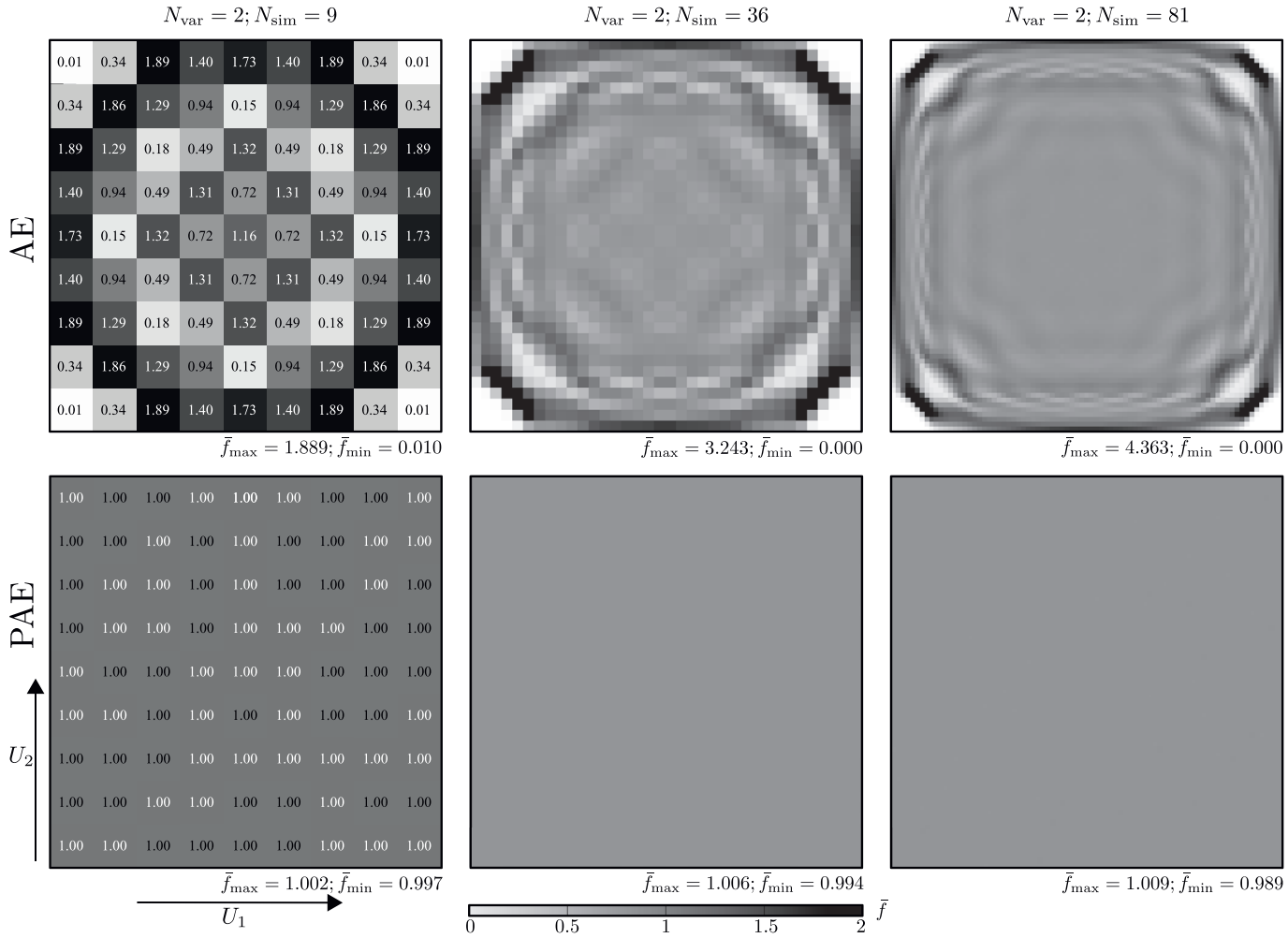

Fig. 3. LHS designs using the original Audze–Eglājs (AE) criterion (top row) and the proposed PAE criterion (bottom row). Relative frequencies $\bar{f}$ calculated from $N_{\text{run}} = 10^7$ designs in the space of $N_{\text{var}} = 2$ variables for different numbers of simulations N_{sim}.

Within the *basic* system (at least one of the points in each pair lies in the original hypercube), let us imagine a set of two points and all its periodic images, $\boldsymbol{u}_i + \boldsymbol{k}_i$ and $\boldsymbol{u}_j + \boldsymbol{k}_j$. Pairs between the original point and its periodic image can apparently be ignored, because they have constant distances and therefore do not influence the minimization of potential energy. We can further limit ourselves only to pairs between the original point $\boldsymbol{u}_i$ and all periodic images of the second point $\boldsymbol{u}_j + \boldsymbol{k}$, because the distance between any omitted pair $L(\boldsymbol{u}_i + \boldsymbol{k}, \boldsymbol{u}_j)$ is repeated in the considered pair of distance $L(\boldsymbol{u}_i, \boldsymbol{u}_j - \boldsymbol{k})$. Among all these pairs, the pair with the *shortest* distance contributes the most to the E^{AE} value. The proposed simplification lies in considering only the *shortest* distance, $\bar{L}_{ij}$, among all these pairs; see the very thick line in Fig. 6 for the case of $N_{\text{var}} = 2$.

The *shortest* distance $\bar{L}_{ij}$ between point $\boldsymbol{u}_i$ and all possible images of point $\boldsymbol{u}_j$ is given by the expression

$$\bar{L}_{ij} = \min_{\boldsymbol{k}}[L(\boldsymbol{u}_i, \boldsymbol{u}_j + \boldsymbol{k})] = \min_{\boldsymbol{k}} \left(\sqrt{\sum_{\nu=1}^{N_{\text{var}}} [\Delta_{ij,\nu} + k_\nu]^2} \right) \tag{7}$$

The problem of searching for the shortest distance can be solved for every coordinate separately thanks to the equalities

$$\begin{aligned} \bar{L}_{ij} &= \min_{\boldsymbol{k}} \left(\sqrt{\sum_{\nu=1}^{N_{\text{var}}} [\Delta_{ij,\nu} + k_\nu]^2} \right) \\ &= \sqrt{\min_{\boldsymbol{k}} \left(\sum_{\nu=1}^{N_{\text{var}}} [\Delta_{ij,\nu} + k_\nu]^2 \right)} \\ &= \sqrt{\sum_{\nu=1}^{N_{\text{var}}} \min_{k_\nu} \left([\Delta_{ij,\nu} + k_\nu]^2 \right)} \end{aligned} \tag{8}$$

where the former equality is valid because the square root function is monotonic and the summation of squares is always positive. The latter equality applies because the optimized parameters k_ν are present separately in separate summands. The problem of finding the nearest image in N_{var}-dimensional space is therefore reduced to N_{var} separate searches of the nearest images in one-dimensional spaces. All the 1D problems always have the form $[\Delta_{ij,\nu} + k_\nu]^2$. The optimal k_ν clearly yields

$$k_\nu = \begin{cases} 0 & \text{if } \Delta_{ij,\nu} \in \langle 0,\ 0.5 \rangle \\ -1 & \text{if } \Delta_{ij,\nu} \in (0.5,\ 1.0 \rangle \end{cases} \tag{9}$$

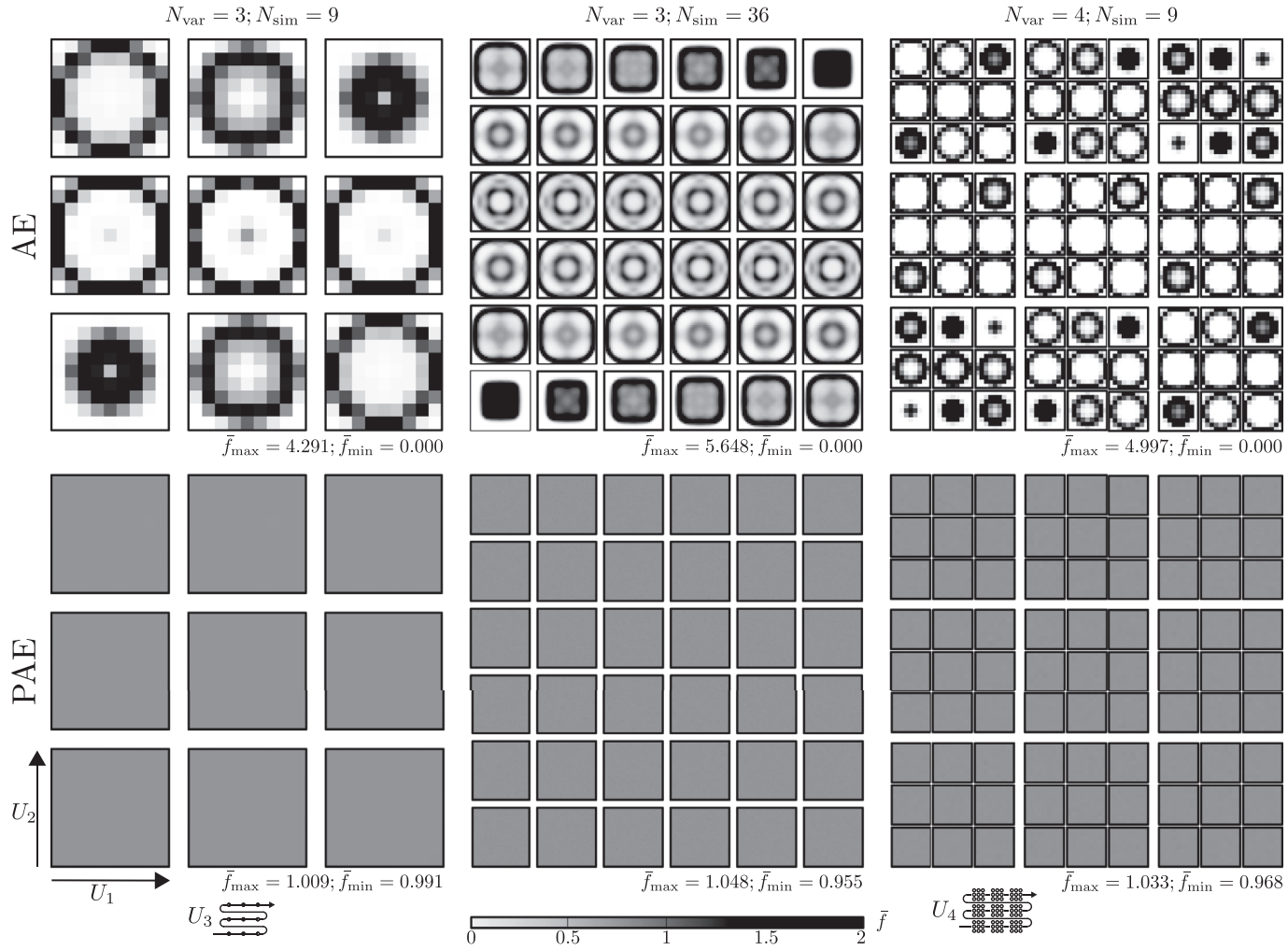

Fig. 4. LHS designs using the original Audze–Eglājs (AE) criterion (top row) and the proposed PAE criterion (bottom row). Relative frequencies $\bar{f}$ calculated from $N_{run} = 10^7$ designs in the space of $N_{var} = 3$ and 4 variables for different numbers of simulations N_{sim}.

and the minimum of each 1D problem ($v = 1, \ldots, N_{var}$) can be expressed as

$$[\overline{\Delta}_{ij,v}]^2 = \min_{k_v} \left([\Delta_{ij,v} + k_v]^2 \right) = [\min \left(\Delta_{ij,v}, \, 1 - \Delta_{ij,v} \right)]^2 \tag{10}$$

Finally, the shortest distance between two points in the periodic space has the following form

$$\overline{L}_{ij} = \sqrt{\sum_{v=1}^{N_{var}} [\overline{\Delta}_{ij,v}]^2} = \sqrt{\sum_{v=1}^{N_{var}} [\min \left(\Delta_{ij,v}, 1 - \Delta_{ij,v} \right)]^2} \tag{11}$$

The simplification made in ignoring all pairs between point $\boldsymbol{u}_i$ and all possible images of point $\boldsymbol{u}_j$ except the nearest one affects the potential energy value. To show in which way the value is modified we present a simple numerical study. Each calculation of potential energy based on the shortest distance only is compared to the potential energy when considering several of the closest images of the second point, $\boldsymbol{u}_j$, in the pair. The number of considered nearest images is controlled by parameter k_{max}. Additional k_{max} layers of images around the nearest point/image are used. The total energy can be expressed as

$$E(k_{max}) = \sum_{\boldsymbol{k} \in \mathcal{K}(k_{max})} \frac{1}{\sum_{v=1}^{N_{var}} \left(\overline{\Delta}_{ij,v} + k_v \right)^2} \tag{12}$$

where $\mathcal{K}(k_{max})$ is a set of all vectors of length N_{var} of integers ranging from $-k_{max}$ to k_{max}. When $k_{max} = 0$, Eq. (11) is recovered. For $k_{max} > 0$, the formula considers $(2 \times k_{max} + 1)^{N_{var}}$ images of the nearest point j contained in $k = 1, \ldots, k_{max}$ surrounding layers of hypercubes around the nearest image (one can imagine k_{max} layers of onions). Fig. 6 shows all nine pairs i, j for $N_{var} = 2$ when $k_{max} = 1$. The thick line shows the distance to the nearest image (layer $k = 0$) and the dashed lines show the next layer around this nearest image.

The study was performed for $N_{var} \in \{1, 2\}$ and the results are shown in Fig. 7. One can see that the difference appears for larger distances between the points; for short distances the majority of the potential energy comes from the closest pair and the difference is negligible. The proposed simplification of the full periodic space to the shortest distance only accentuates the pairs with shorter distance, i.e. one can think about the simplification as a modification of the repulsive force-distance relationship between the points.

When k_{max} reaches infinity, infinitely many periodic repetitions are considered. Though images in distant layers (high k) do not contribute much to the criterion as the distance between the points becomes high, the number of such images in the kth layer grows rapidly. Our calculations suggest that for $N_{var} > 1$, the energy in Eq. (12) tends to infinity with increasing k_{max}.

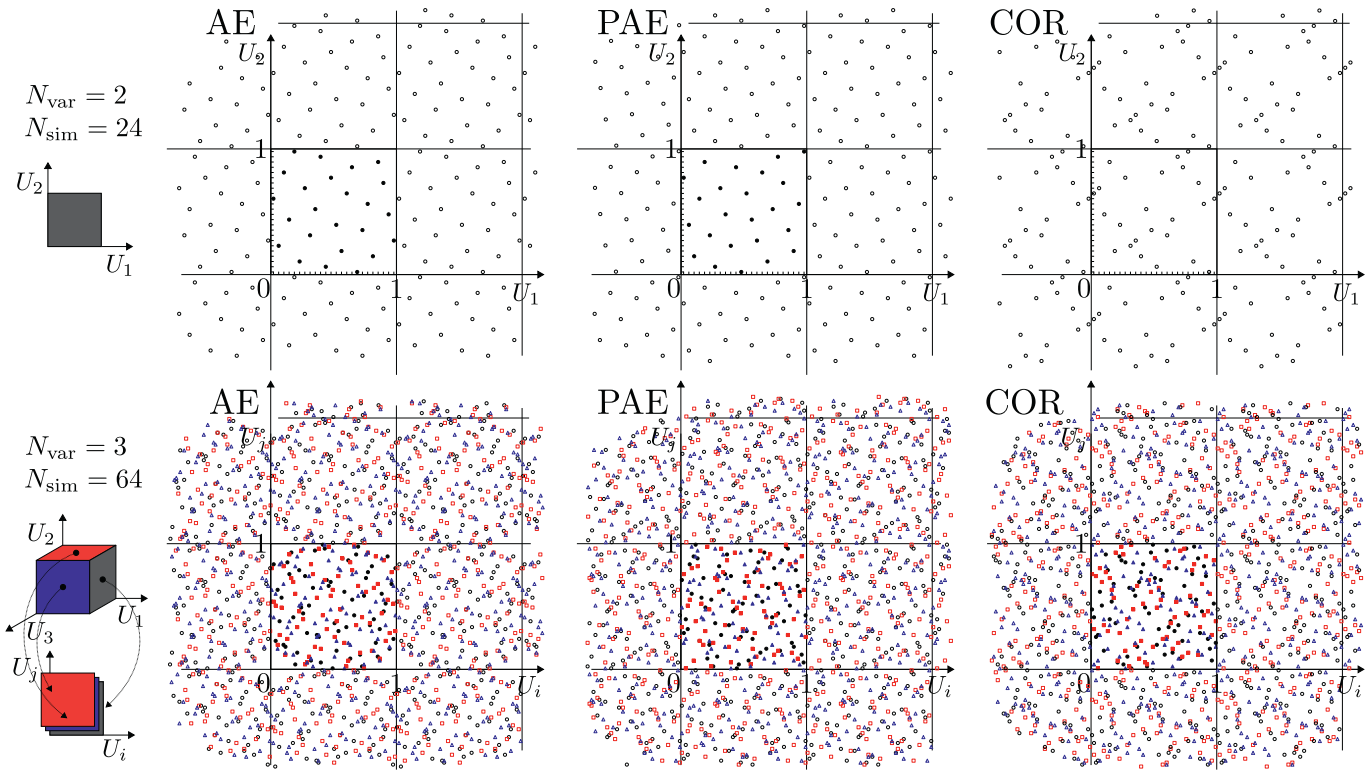

Fig. 5. Comparison of optimized LH-sampling points selected from uniform density with independent marginals, optimized via three criteria. Top row: 2D domain, $N_{sim} = 24$. Bottom row: 3D domain, $N_{sim} = 64$ (the three different projections of points are plotted in a single bivariate scatterplot with different symbols). Left: original AE criterion [1,3]; middle: proposed PAE criterion; right: correlation criterion [57].

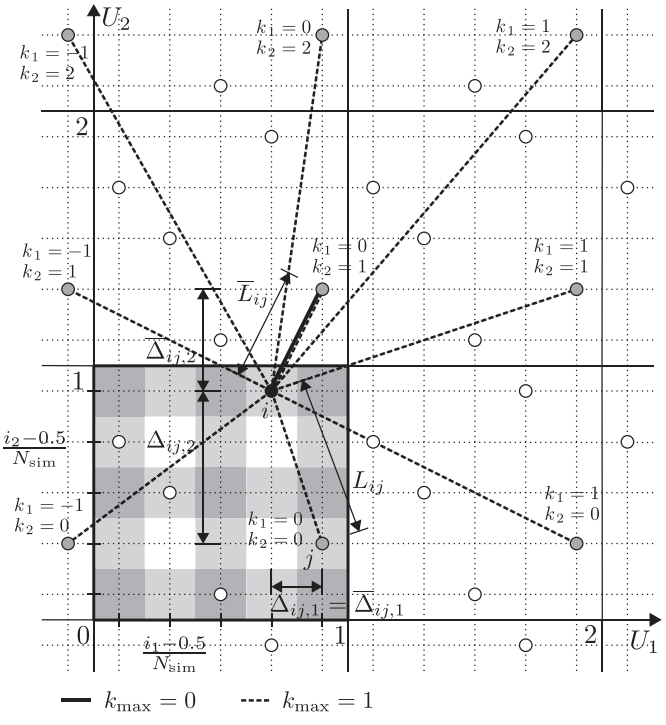

Fig. 6. Periodic space, the shortest distance $\overline{L}_{ij}$ and all pairs in the first layer around point $\boldsymbol{u}_i$.

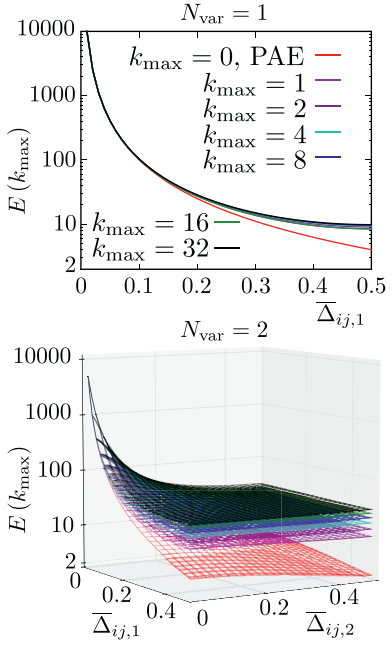

Fig. 7. Difference in the potential energy of a system when considering the first k_{max} periodic images; top: $N_{var} = 1$, bottom: $N_{var} = 2$.

6. Uniformity of the proposed Periodic Audze-Eglājs criterion

Motivated by the observation described in the previous section, an improvement of the AE criterion is proposed. To distinguish between the original AE formulation [1] and the proposed one based on periodic space, we will call the new formulation the Periodic

Audze-Eglājs (PAE) criterion. The proposed PAE criterion has the following form

$$E^{\mathrm{PAE}} = \sum_{i=1}^{N_{\mathrm{sim}}} \sum_{j=i+1}^{N_{\mathrm{sim}}} \frac{1}{\bar{L}_{ij}^2},$$
$$\bar{L}_{ij}^2 = \sum_{v=1}^{N_{\mathrm{var}}} [\min\left(\Delta_{ij,v},\, 1-\Delta_{ij,v}\right)]^2 \tag{13}$$

By comparing Eq. (13) with the original formulation in Eq. (3) one can see that the only difference between them lies in selecting the minima between $(\Delta_{ij,v})$ and $(1-\Delta_{ij,v})$ along each coordinate $v \in \langle 1, N_{\mathrm{var}}\rangle$ instead of using the coordinate difference $(\Delta_{ij,v})$ directly. Technically, this improvement is very easy to implement in computer programs and the additional computer time necessary to perform the comparison and selection of the minima is inconsiderable. We suggest using the effective algorithm based on the matrix $\boldsymbol{T}$ described in Section 3.

Figs. 3 and 4 bottom clearly demonstrate that the new formulation provides *uniform* designs; the figures provide a direct comparison with the biased behavior of the AE criterion (the same numerical example settings were used for the AE and PAE demonstration).

The source of uniformity actually lies in the *invariance of PAE with respect to translation*. If all the points in periodic space are shifted by an arbitrary vector, the PAE value remains unchanged. Therefore, when generating the experimental points, even if there is a tendency to form some pattern, the pattern is always randomly shifted and sampling becomes *uniform*. It is simple to show the invariance with respect to translation; it can be proven separately using 1D problems because the $\overline{\Delta}_{ij,v}$ is already invariant under translation by arbitrary r_v. Let us imagine two points with the coordinates $x_{i,v}$ and $x_{j,v}$ with $\Delta_{ij,v} = |x_{i,v} - x_{j,v}|$; see Eq. (2). As the coordinates $x_{i,v} + r_v$ and $x_{j,v} + r_v$ are simultaneously translated by r_v, nothing happens until both of them remain in the interval $\langle 0, 1\rangle$ because the projected distance remains constant $\Delta^+_{ij,v} = \Delta_{ij,v}$. When one of the points exceeds the domain boundary given by value 1 (or 0), the exceeding point becomes a periodic image and the original point enters the domain through the opposite side. The projected distance between the shifted pair of points becomes $\Delta^+_{ij,v} = 1 - \Delta_{ij,v}$. However, the periodic projected distance remains the same

$$\begin{aligned}\overline{\Delta}^+_{ij,v} &= \min(\Delta^+_{ij,v}, 1-\Delta^+_{ij,v}) \\ &= \min(1-\Delta_{ij,v}, 1-1+\Delta_{ij,v}) \\ &= \min(1-\Delta_{ij,v}, \Delta_{ij,v}) = \overline{\Delta}_{ij,v}\end{aligned} \tag{14}$$

Therefore, even if the whole design is shifted by a random distance r_v in any direction v, the proposed periodic criterion remains unchanged.

7. Sets of optimal solutions

The relative frequency maps presented in Figs. 3 and 4 need some additional comments. The Figures were obtained with a heuristic combinatorial optimization algorithm that does not necessarily deliver arrangements corresponding to the global minimum of the objective function. In fact, the N_{run} solutions used to plot the histograms have been obtained with a set of parameters (called cooling schedule, see Vořechovský and Novák [57]) that deliver solutions in relatively short time. The cooling schedule strongly influences how close the final AE criterion (objective function) is to its global minimum.

For low numbers of sampling points, N_{sim}, and a low dimensionality of the design space, N_{var}, it is easy to check all $(N_{\mathrm{sim}}!)^{N_{\mathrm{var}}-1}$ possible mutual permutations and select the one(s) delivering the lowest possible value of the objective function. For example, the case with $N_{\mathrm{sim}} = 9$ and $N_{\mathrm{var}} = 2$ has only two optimal solutions (one can be obtained from the other by flipping the design around the central horizontal or vertical line). The lower bound on LHS-AE design equals $E^{\mathrm{AE}}(9,2) = 156.735$. The frequency map obtained with these two best possible designs as well as these two optimal designs are plotted in Fig. 8 left. Acceptance of all solutions having AE criterion less or equal to 158, 159, 160 or 175 leads to 4, 8, 16 or 6794 possible solutions, respectively. The frequency maps for these solutions are shown in Fig. 8 center (only the symmetrical quarters of the design space are plotted). By further relaxation of the acceptance level of AE with respect to its lower bound, the pool of solutions gets richer and the maps approach uniform distribution.

Let us note that there is no acceptance level that delivers figure identical to Fig. 3 top left. The reason is that the heuristic algorithm does not consider all possible solutions satisfying the condition with equal probability (while the exhaustive search does). The algorithm merely delivers solutions obtained with a certain cooling schedule and the solutions satisfying an acceptance level are not equally likely to be discovered.

Similarly, the other tested configurations can be shown to deliver sharper frequency maps that document the nonuniformity of the coverage of the design space, e.g. for $N_{\mathrm{sim}} = 9$ and $N_{\mathrm{var}} = 3$ exists 24 optimal solutions with criterion $E^{\mathrm{AE}}(9,3) = 78.653$. Exhausting all possible configurations in larger dimensions and for larger N_{sim} becomes too computationally demanding, though.

On the other hand, the proposed periodic version of the criterion provides sets of optimal solution that always provide uniform distribution. The reason lies in the invariance of the PAE with respect to translation (see Section 6); accepting one design implies acceptance of all its possible shifts. Note that when using LHS, there are $N_{\mathrm{sim}}{}^{N_{\mathrm{var}}}$ possible shifts. Set of optimal solutions for LHS-PAE design for $N_{\mathrm{sim}} = 9$ and $N_{\mathrm{var}} = 2$ contains 324 possible solution ($E^{PAE}(9,2) = 245.732$), among which only four are unique. This means that all 324 optimal designs can be obtained by shifting one of these 4 unique solutions in one or two directions. The frequency map and unique solutions are shown in Fig. 8 right. The four unique solutions are surprisingly not symmetrical. Nevertheless, every optimal solution (including the four unique ones) has its symmetrical plans obtained by shifting one of these unique solutions. For $N_{\mathrm{sim}} = 9$ and $N_{\mathrm{var}} = 3$ the PAE criterion provides 648 optimal solutions with criterion $E^{PAE}(9,3) = 131.143$.

8. Application to statistical analyses of functions of independent random variables

As mentioned above, one of the frequent uses of DoE is in *statistical sampling* for Monte Carlo integration. We present the application of statistical sampling to the problem of estimating statistical moments of a function of random variables. In particular, a deterministic function, $Z = g(\boldsymbol{X})$, is considered, which can be a computational model or a physical experiment. Z is the uncertain response variable (or generally a vector of the outputs). The vector $\boldsymbol{X} \in \mathbb{R}^{N_{\mathrm{var}}}$ is considered to be a random vector of N_{var} continuous marginals (input random variables describing uncertainties/randomness) with a given joint probability density function (PDF).

Estimation of the statistical moments of variable $Z = g(\boldsymbol{X})$ is, in fact, an estimation of integrals over domains of random variables weighted by a given joint PDF of the input random vector $f_{\boldsymbol{X}}(\boldsymbol{x})$. We seek the statistical parameters of $Z = g(\boldsymbol{X})$ in the form of the following integral:

$$\mathrm{E}[S[g(\boldsymbol{X})]] = \int_{-\infty}^{\infty} \cdots \int_{-\infty}^{\infty} S[g(\boldsymbol{x})]\, \mathrm{d}F_{\boldsymbol{X}}(\boldsymbol{x}) \tag{15}$$

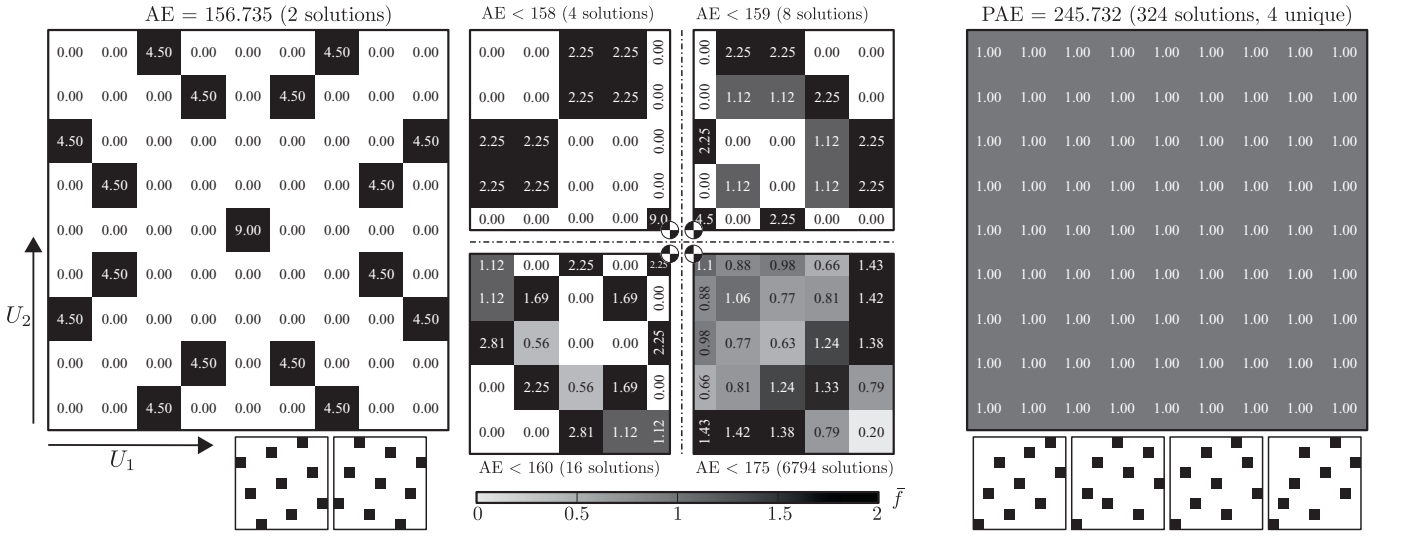

Fig. 8. Relative frequencies $\bar{f}$ calculated of LH-sample sets with Audze-Eglajs (AE) criterion and its proposed periodic version (PAE) for $N_{\text{sim}} = 9$ and $N_{\text{var}} = 2$. These maps are constructed from sets of optimal solutions (left for AE, right for PAE), or all solutions having AE criterion lower than 158, 159, 160 and 175 (center). The scatterplots of designs plotted at the bottom are two optimal designs for AE and four unique optimal designs for PAE.

where $\mathrm{d}F_{\boldsymbol{X}}(\boldsymbol{x}) = f_{\boldsymbol{X}}(\boldsymbol{x}) \cdot \mathrm{d}x_1\, \mathrm{d}x_2 \cdots \mathrm{d}x_{N_{\text{var}}}$ is the infinitesimal probability ($F_{\boldsymbol{X}}$ denotes the joint cumulative density function) and where the particular form of the function $S[g(\,\cdot\,)]$ depends on the statistical parameter of interest. To gain the mean value, $S[g(\cdot)] = g(\cdot)$; higher statistical moments of the response can be obtained by integrating polynomials of $g(\,\cdot\,)$. The probability of failure (an event defined as $g(\,\cdot\,) < 0$) is obtained in a similar manner; $S[\,\cdot\,]$ is replaced by the Heaviside function (or indicator function) $H[-g(\boldsymbol{X})]$, which equals one for a failure event ($g < 0$) and zero otherwise. In this way, the domain of integration of the PDF is limited to the failure domain.

In Monte Carlo sampling, which is the most prevalent statistical sampling technique, the above integrals are numerically estimated using the following procedure:

(i) draw N_{sim} realizations of $\boldsymbol{X}$ that share the same probability of occurrence $1/N_{\text{sim}}$ by using its joint distribution $f_{\boldsymbol{X}}(\boldsymbol{x})$ (the points are schematically illustrated by the rows in Fig. 1 left);
(ii) compute the same number of output realizations of $S[g(\,\cdot\,)]$; and
(iii) estimate the desired parameters as arithmetical averages. We now limit ourselves to independent random variables in vector $\boldsymbol{X}$. The aspect of the correct representation of the target joint PDF of the inputs mentioned in item (i) is absolutely crucial. Practically, this can be achieved by reproducing a *uniform distribution* in the design space (unit hypercube) that represents the space of sampling probabilities.

Assume now a vector random variable $\boldsymbol{U}$ that is selected from a multivariate uniform distribution in such a way that its independent marginal variables U_ν, $\nu = 1, \ldots, N_{\text{var}}$, are uniform over intervals (0; 1). A vector with such a multivariate distribution is said to have an "independence copula" [36]

$$C(u_1, \ldots, u_{N_{\text{var}}}) = \mathrm{P}(U_1 \le u_1, \ldots, U_{N_{\text{var}}} \le u_{N_{\text{var}}}) = \prod_{\nu=1}^{N_{\text{var}}} u_\nu \tag{16}$$

These uniform variables can be seen as sampling probabilities: $F_{X_\nu} = U_\nu$. The joint cumulative distribution function then reads $F_{\boldsymbol{X}}(\boldsymbol{x}) = \prod_\nu F_{X_\nu} = \prod_\nu U_\nu$, and $\mathrm{d}F_{\boldsymbol{X}}(\boldsymbol{x}) = \prod_\nu \mathrm{d}U_\nu$. The individual random variables can be obtained by inverse transformations

$$\{X_1, \ldots, X_{N_{\text{var}}}\} = \{F_1^{-1}(U_1), \ldots, F_{N_{\text{var}}}^{-1}(U_{N_{\text{var}}})\} \tag{17}$$

and similarly the realizations of the original random variables are obtained by the component-wise inverse distribution function of a point $\boldsymbol{u}$ (a realization of $\boldsymbol{U}$) representing a sampling probability

$$\boldsymbol{x} = \{x_1, \ldots, x_{N_{\text{var}}}\} = \{F_1^{-1}(u_1), \ldots, F_{N_{\text{var}}}^{-1}(u_{N_{\text{var}}})\} \tag{18}$$

With the help of this transformation from the original to a uniform joint PDF, the above integral in Eq. (15) can be rewritten as

$$\mathrm{E}[S[g(\boldsymbol{X})]] = \int_0^1 \cdots \int_0^1 S[g(\boldsymbol{x})]\, \mathrm{d}C(u_1, \ldots, u_{N_{\text{var}}}) = \int_{[0,1]^{N_{\text{var}}}} S[g(\boldsymbol{x})] \prod_{\nu=1}^{N_{\text{var}}} \mathrm{d}U_\nu \tag{19}$$

so that the integration is performed over a unit hypercube with uniform unit density.

We now assume an estimate of this integral by the following statistic (the average computed using N_{sim} realizations of $\boldsymbol{U}$, namely the sampling points $\boldsymbol{u}_i$ $(i = 1, \ldots, N_{\text{sim}})$)

$$\mathrm{E}[S[g(\boldsymbol{X})]] \approx \frac{1}{N_{\text{sim}}} \sum_{i=1}^{N_{\text{sim}}} S[g(\boldsymbol{x}_i)] \tag{20}$$

where the sampling points $\boldsymbol{x}_i = \{x_{i,1}, \ldots, x_{i,\nu}, \ldots, x_{i,N_{\text{var}}}\}$ are selected using the transformation in Eq. (18), i.e. $x_{i,\nu} = F_\nu^{-1}(u_{i,\nu})$, in which we assume that each of the N_{sim} sampling points $\boldsymbol{u}_i$ $(i = 1, \ldots, N_{\text{sim}})$ were selected with the same probability of $1/N_{\text{sim}}$. Violation of the uniformity of the distribution of points $\boldsymbol{u}_i$ in the unit hypercube may lead to erroneous estimations of the integrals. We will show that the original definition of the AE criterion suffers from this problem.

This section continues with three numerical examples presenting three transformations of standard independent Gaussian random variables X_ν, $\nu = 1, \ldots, N_{\text{var}}$. The non-uniformity of the original AE criterion and also the improved performance of the proposed PAE criterion will be demonstrated by showing the ability of the optimized samples to estimate the mean value, standard deviation, skewness and excess kurtosis (denoted as μ_Z, σ_Z, γ_Z and κ_Z) of the transformed variable $Z = g(\boldsymbol{X})$.

8.1. Numerical examples

We consider three functions (transformations of input random variables):

$$Z_{\text{sum}} = g_{\text{sum}}(\boldsymbol{X}) = \sum_{\nu=1}^{N_{\text{var}}} X_\nu^2 \tag{21}$$

$$Z_{\text{exp}} = g_{\text{exp}}(\boldsymbol{X}) = \sum_{\nu=1}^{N_{\text{var}}} \exp\left(-X_\nu^2\right) \tag{22}$$

$$Z_{\text{prod}} = g_{\text{prod}}(\boldsymbol{X}) = \prod_{\nu=1}^{N_{\text{var}}} X_\nu \tag{23}$$

where the input variables X_ν, $\nu = 1, \ldots, N_{\text{var}}$ are independent standard Gaussian variables.

The first random variable Z_{sum} has a chi-squared distribution (also chi-square or χ^2-distribution) with N_{var} degrees of freedom. The standard deviation of this distribution is well known: $\sigma_{\text{sum}} = \sqrt{2N_{\text{var}}}$. The chi-squared distribution slowly converges to a Gaussian distribution as N_{var} grows large.

The second random variable Z_{exp} has the exact statistical moments derived in Appendix B. The approximate standard deviation is $\sigma_{\text{exp}} \approx 0.337\,461\,\sqrt{N_{\text{var}}}$ and approximate skewness is $\gamma_{\text{exp}} \approx -0.305\,281/\sqrt{N_{\text{var}}}$.

The third variable Z_{prod} has a probability density function symmetrical about zero. The exact form of the PDF together with formulas for the first four statistical moments are derived in Appendix C. The standard deviation of Z_{prod} equals: $\sigma_{\text{prod}} = 1$ and the excess kurtosis equals: $\kappa_{\text{prod}} = 3^{N_{\text{var}}} - 3$.

8.2. Discussion of results

The quality of sampling is measured through the difference between the theoretical and estimated statistical parameters of Z. Since the placement of N_{sim} design points into an N_{var}-dimensional hypercube is random (it depends on sequences generated by a pseudo-random number generator), the estimated statistical parameter can also be viewed as a realization of a random variable. The simulated annealing algorithm [57] has been used for the optimization of the mutual ordering of LH samples for three DoE criteria: AE, PAE and COR (Pearson's correlation coefficient). A relatively high number of $N_{\text{run}} = 10^3$ designs were optimized for the same settings (criterion, N_{sim} and N_{var}) and the mean value and standard deviation of the estimated statistical parameters have been plotted in the form of graphs – dependencies on the sample size N_{sim}; see Figs. 9–11. The graphs show the exact solution for each selected statistical parameter via a dashed line. The average result of its estimation is plotted by a solid line surrounded by a scatter-band representing the average ± one standard deviation. Such graphs give an idea about the convergence of the average estimation and also the variance of the estimation. Crude Monte Carlo results are not presented as the estimates exhibit a large variance. In LHS, the variability of the estimate is never higher than in crude Monte Carlo sampling because the selection of sampling probabilities is deterministic and the only variability arises from random mutual pairing.

The ability to estimate the mean value is purposely not presented. The reason is that samples optimized with all three criteria (COR, AE and PAE) provide exactly the same estimates of μ_{sum} and μ_{exp}. These estimates have no variability as the functions are additive and, in the LHS method, the averages are independent of the mutual ordering of coordinates. For the last function, g_{prod}, the estimated mean values are slightly different (different variances) but the results for the second and fourth central moments are much more convincing. The product function $g_{\text{prod}}(\boldsymbol{X})$ is selected intentionally because the results are extremely sensitive to variations between different LHS designs. That is why the results (σ_{prod} and κ_{prod}) exhibit a large amount of variability.

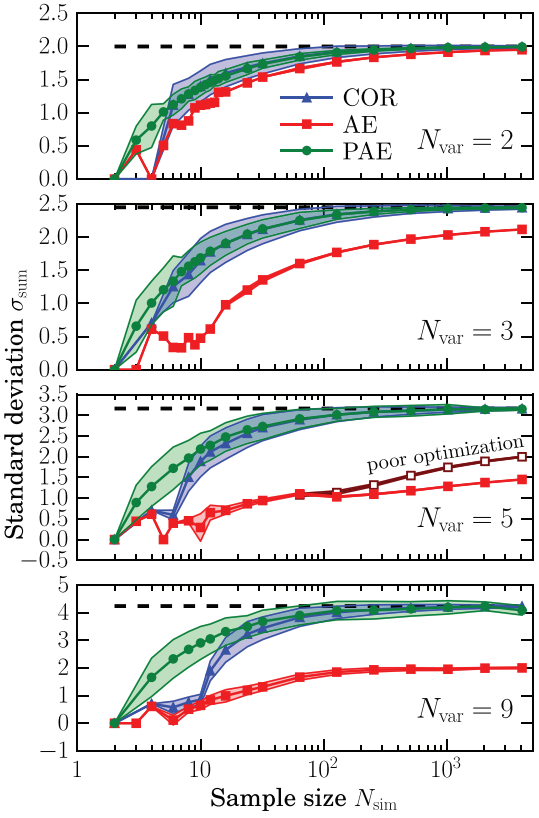

Fig. 9. Z_{sum}: convergence of the estimated standard deviation σ_{sum} for various numbers of variables N_{var} with increasing sample size N_{sim}.

The general trends are as follows:

- The AE criterion yields, on average, erroneous estimates (with almost no variability) for the studied statistical characteristics of the investigated three g functions. The error becomes pronounced for higher N_{var}. Increasing the sample size N_{sim} does not help. Both the incorrect means and the low variance of estimates are consequences of *non-uniform* sampling: some regions are under-represented (such as corners) and others are over-represented (as documented in Figs. 3 and 4 where the AE-optimized sampling points occur only in hyper-spheres inside the hypercube).
- The PAE criterion yields a uniform distribution of points and therefore the estimators converge to the exact values.
- The COR criterion yields a uniform distribution of points for $N_{\text{sim}} \to \infty$; however, for small N_{sim} the algorithm selects from a limited number of optimal arrangements [55] that are not uniform.
- Estimates obtained with PAE are, on average, never worse than with COR – in most of the cases they are better. Also, the variance of the estimates obtained with PAE is usually lower than that gained from COR. In other words, the estimates converge faster with smaller variance.

The best of the three methods seems to be the PAE criterion. One can argue that for the product function in $N_{\text{var}} = 5$ dimensions, the variance of PAE estimates are as high as in the case of COR. However, this is an inevitable consequence of the high sensitivity of the function selected. For example, the placement of just one point into a corner of the hypercube (u_i equals either $0.5/N_{\text{sim}}$

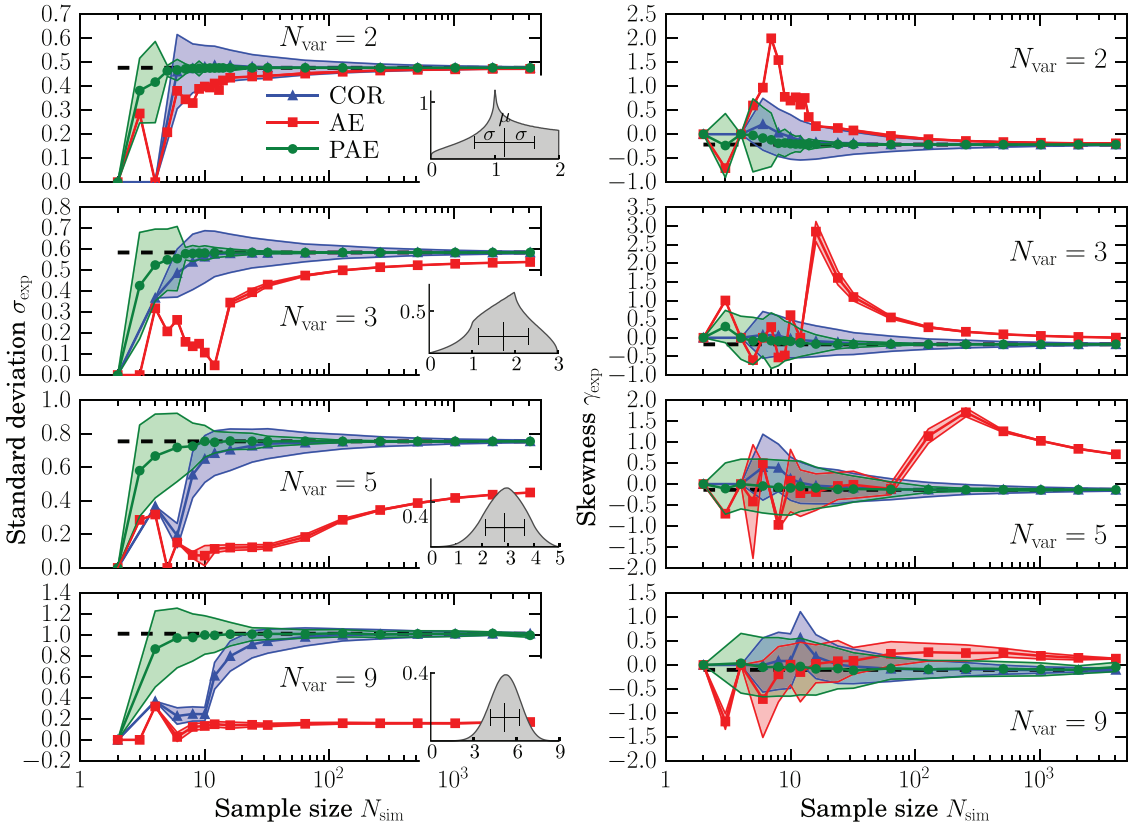

Fig. 10. Z_{exp}: convergence of estimated σ_{exp} and γ_{exp} with increasing sample size N_{sim}. The insets visualize the PDF of Z_{exp}.

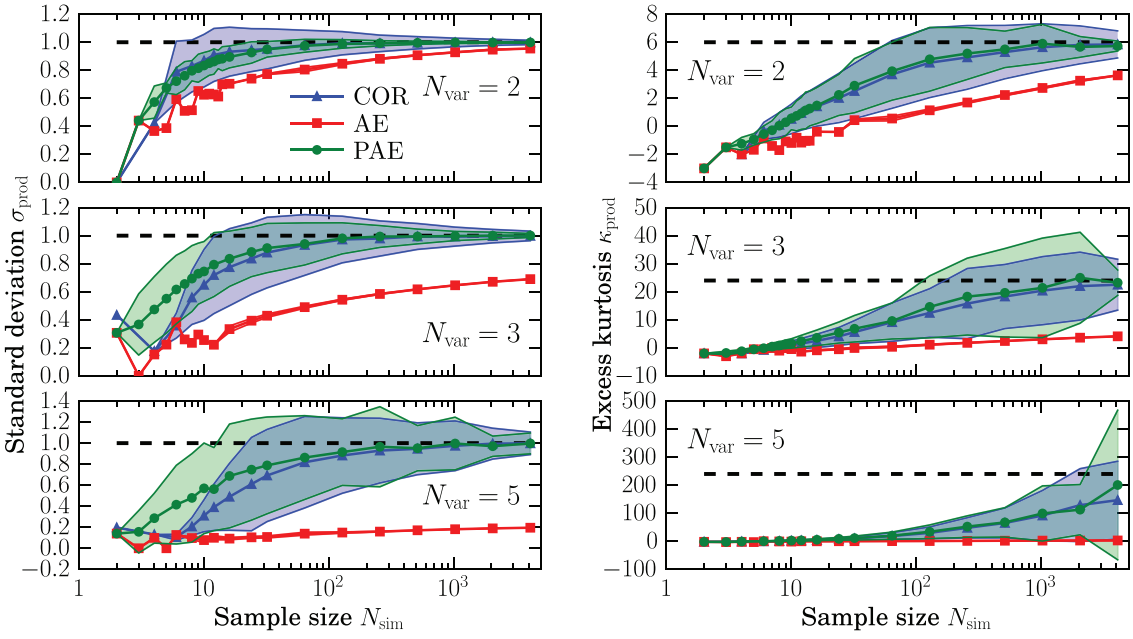

Fig. 11. Z_{prod}: comparison of the convergence of estimated σ_{prod} and κ_{prod} with increasing sample size N_{sim}.

or $1 - 0.5/N_{\text{sim}}$) results in an extremely high or low result for the estimated product g. We remind the reader that the original AE criterion suppresses these regions completely.

The results of skewness γ_{exp} show the strange behavior of AE-optimized designs. We believe that this strange behavior is again a consequence of the AE criterion forcing the points into a subregion inside the hypercube. The subregion changes its shape gradually with increasing N_{sim} and the estimates gradually evolve into different values.

The estimates of the standard deviation of all three functions (σ_{sum}, σ_{exp} and σ_{prod}) obtained for very small sample sizes N_{sim} show almost no variance in the case of AE and COR criteria. This is

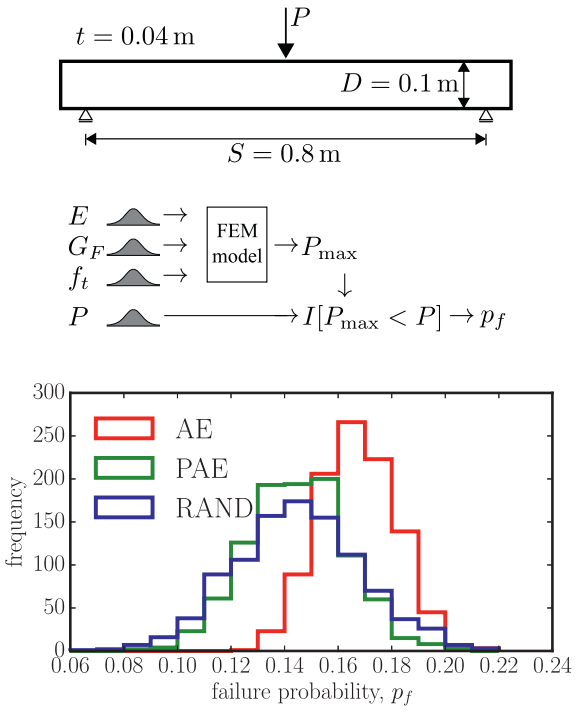

Fig. 12. Evaluation of failure probability of a concrete beam. Top: sketch of the model and dimensions; center: scheme of the calculation; bottom: histograms of estimated failure probability obtained with samples of $N_{\text{sim}} = 100$ and based on $N_{\text{run}} = 1000$ repetitions.

because the heuristic algorithm of simulated annealing is still able to check all $(N_{\text{sim}}!)^{N_{\text{var}}-1}$ different designs (mutual orderings). For the AE and COR criteria, the optimal designs form a small number of (nonuniform) structures and the estimates of the statistical parameters are identical (the number of COR-optimal solutions has been studied in [55]). The PAE criterion, however, does not lead to such strange structures and the parameters are estimated better (on average) but with higher variance.

The graphs in Figs. 9–11 present the results for LHS-optimized designs. The same trends have been observed for MC-AE and MC-PAE designs in which the sets of coordinates for each variable have been sampled by crude Monte Carlo and the pairing have later been optimized by AE or PAE. The only difference is that MC samples produce higher variance of the estimators.

The presented inability of LHS-AE optimized samples to deliver unbiased estimates of the desired statistical parameters is more pronounced when the optimization of samples discovers the best possible solutions, see Section 7. The fact that the cooling schedule was used with relatively mild requirements helped the LHS-AE samples to show themselves as better than they really are. This effect is pronounced for higher N_{sim} and N_{var} where the designs used for integration must be far from actual optimal designs. This is documented in Fig. 9, $N_{\text{var}} = 5$ where there is an additional curve obtained using poor optimization settings.

9. Engineering example

The examples analyzed in Section 8.1 are simple and it is easy to solve the transformations analytically. In order to demonstrate the differences between sampling plans generated by AE and PAE on some complex engineering problem, the paper presents analysis of the failure probability of a concrete beam loaded in three-point-bending. Fig. 12 shows a computational model of the beam with depth 0.1 m, span 0.8 m and thickness 0.04 m. Four independent random variables ($N_{\text{var}} = 4$) are considered: the elastic modulus E (with mean $\mu_E = 30$ GPa), tensile strength f_t ($\mu_{f_t} = 3$ MPa), fracture energy G_F ($\mu_{G_F} = 80\,\text{Jm}^{-2}$) and load action P ($\mu_P = 1.4$ kN). All the random input parameters are assumed to be normally distributed with the coefficient of variation of 20%. The loading capacity of the beam, $P_{\max}$, is obtained using OOFEM software [39,40], the non-linear finite element solver. The isotropic damage model with Mazar's equivalent strain [29] and linear softening is used. The nonlinear calculation represents a function – transformation of three random variables: $P_{\max} = g_{P_{\max}}(E, f_t, G_F)$. The loading force is compared to the load capacity and either failure ($P_{\max} < P$) or success is detected via indicator function $I[P_{\max} < P]$ returning 1 when the condition is fulfilled, and zero otherwise. The failure probability, p_f, is estimated based on $N_{\text{sim}} = 100$ simulations as

$$p_f \approx \frac{1}{N_{\text{sim}}} \sum_{i=1}^{N_{\text{sim}}} I[P_{\max}(E, f_t, G_F) < P] \tag{24}$$

To get idea about the variance of such estimator, the calculation of p_f is repeated $N_{\text{run}} = 1000$ times and Fig. 12 bottom shows the histogram of the estimated 1000 failure probabilities. When the LH-sampling plan is optimized with the original AE formulation, the calculation is wrong and predicts, on average, too high $\mu_{p_f} = 0.1622$. Using the proposed periodic version (PAE), the mean μ_{p_f} is 0.1400 which corresponds to the reference case of random LH-sampling plan without any optimization (RAND), with the same mean of 0.1400. One can also see that the RAND estimator has somewhat greater variance than the proposed PAE estimator (the coefficient of variation in the RAND case is 0.171 compared to 0.134 obtained with PAE). This variance reduction confirms that the PAE-optimized design has a better selection of integration points compared to a random ordering. The original AE formulation delivers wrong results.

10. Conclusions

It has been shown that the original Audze-Eglājs criterion used for optimization of the Design of Experiments provides a *nonuniform* experimental point distribution. Even though this feature is not important in several applications of Design of Experiments, it is the crucial property in numerical Monte-Carlo type integration. Similarly, the correlation criterion of optimization (COR) also yields nonuniform coverage of the design domain; however, the problem disappears when sample size N_{sim} increases. Violation of uniformity leads to significant errors in integral estimates, as demonstrated in this paper. Since the widely used AE criterion samples more frequently in some subregions of the design domain while leaving other areas under-represented, numerical integration using the AE criterion provides incorrect results.

A simple remedy based on considering the periodicity of the design space was proposed, and it was demonstrated that the modified version – the Periodic Audze-Eglājs (PAE) criterion – provides a truly uniform distribution of points in the design domain. The PAE and AE criteria have the same computational complexity, so no additional effort is associated with considering the proposed scheme. The proposed PAE criterion is invariant with respect to shifts of the whole sample in any direction.

The numerical studies presented in this paper were performed with Latin Hypercube Samples (optimized using different criteria). However, the criticism of the AE criterion and the remedy using the proposed PAE criterion also holds for crude Monte Carlo Sampling (independent sampling on the $\langle 0, 1\rangle$ interval).

The proposed PAE criterion controls the optimality of point distribution in N_{var}-dimensional space. Additionally, using LHS (a stratified sampling scheme) guarantees a perfectly regular grid of points projected into separate dimensions $v = 1, \ldots, N_{\text{var}}$. The

optimality of the projections into higher dimensional subspaces (dimensions $2, \ldots, N_{\text{var}} - 1$) is not considered by the PAE.

The proposed criterion is implemented in FReET software [38]. It has also been implemented for the optimization of a sample in the sample size extension of an existing LH sample (a method proposed in [56]).

Acknowledgments

The authors acknowledge financial support provided by the Czech Science Foundation under project no. 16-22230S. Additionally, the second author acknowledges support under project no. GA15-07730S.

Appendix A. Non-uniformity of the original AE criterion

In this appendix, we propose an argument explaining the tendency of the original AE criterion to produce a non-uniform distribution of points in the design space. Let us assume an existing design ($N_{\text{var}} = 2$) that is considered to be uniform. The coordinates along each individual direction are fixed, but the mutual ordering can be changed. These coordinates can be obtained by MC or LH sampling or any other convenient method. Suppose that there exist a point $\boldsymbol{a} = (u_{a,1}, u_{a,2})$ in the bottom left corner, i.e. there is no point with lower horizontal coordinate (U_1) or lower vertical coordinate (U_2). Consider also the point $\boldsymbol{b} = (u_{b,1}, u_{b,2})$ with the second lowest horizontal coordinate U_1. We will show that it is more convenient (in a statistical sense) to swap the first coordinate of $\boldsymbol{a}$ and $\boldsymbol{b}$ so that in the new configuration point $\bar{\boldsymbol{a}}$ will move outside the corner and point $\bar{\boldsymbol{b}}$ will have minimal U_1. Therefore, the AE criterion will systematically choose designs with empty corners.

The situation is sketched in Fig. 13 left: the two gray areas $\mathcal{A}$ and $\mathcal{B}$ represent regions containing the remaining points. The total value of the AE criterion for the original design is given by (i) pairs between points in the gray areas: $\mathcal{AA}$, $\mathcal{BB}$ and $\mathcal{AB}$; (ii) pairs between point $\boldsymbol{a}$ and the gray areas: $\boldsymbol{a}\mathcal{A}$, $\boldsymbol{a}\mathcal{B}$; (iii) pairs between point $\boldsymbol{b}$ and the gray areas: $\boldsymbol{b}\mathcal{A}$, $\boldsymbol{b}\mathcal{B}$; (vi) pair $\boldsymbol{ab}$. The AE criterion value for the modified design is given by the same structure, except points $\boldsymbol{a}$ and $\boldsymbol{b}$ are replaced by $\bar{\boldsymbol{a}}$ and $\bar{\boldsymbol{b}}$. Therefore:

- The contribution of all pairs within domains $\mathcal{AA}$, $\mathcal{BB}$ and $\mathcal{AB}$ remains unchanged;
- The contribution of pair $\boldsymbol{ab}$ equals the contribution of the modified pair $\bar{\boldsymbol{a}}\bar{\boldsymbol{b}}$ because both pairs have the same distance;
- We suppose that the contribution of a set of pairs $\boldsymbol{a}\mathcal{A}$ ($\boldsymbol{b}\mathcal{A}$) statistically equals to contribution of a set $\bar{\boldsymbol{b}}\mathcal{A}$ ($\bar{\boldsymbol{a}}\mathcal{A}$, respectively); These two areas are supposed to have a uniform distribution of points and after the coordinate exchange the situation is symmetrical with respect to the horizontal axis through the center of region $\mathcal{A}$
- The only difference then comes from a set of pairs in $\boldsymbol{b}\mathcal{B}$, which is changed to $\bar{\boldsymbol{b}}\mathcal{B}$, and $\boldsymbol{a}\mathcal{B}$, which is changed to $\bar{\boldsymbol{a}}\mathcal{B}$.

Now, we need to show that $E^{\text{AE}}(\boldsymbol{b}\mathcal{B}) + E^{\text{AE}}(\boldsymbol{a}\mathcal{B}) > E^{\text{AE}}(\bar{\boldsymbol{b}}\mathcal{B}) + E^{\text{AE}}(\bar{\boldsymbol{a}}\mathcal{B})$. If this holds, we prove that the modified design is preferable and the AE criterion avoids the corner point $\boldsymbol{a}$. We will demonstrate validity of even stronger statement, namely that this is valid for *any point* from $\mathcal{B}$. Let $\boldsymbol{c}$ be an arbitrary point from region $\mathcal{B}$ at coordinates $\left(u_{b,1} + \Delta_{bc,1}, u_{b,2} + \Delta_{bc,2}\right)$; we can show that $E^{\text{AE}}(\boldsymbol{bc}) + E^{\text{AE}}(\boldsymbol{ac}) > E^{\text{AE}}(\bar{\boldsymbol{b}}\boldsymbol{c}) + E^{\text{AE}}(\bar{\boldsymbol{a}}\boldsymbol{c})$. Rewriting the AE contributions of considered pairs, we would like to show that

$$\frac{1}{L_{\bar{a}c}^2} + \frac{1}{L_{bc}^2} > \frac{1}{L_{\bar{a}c}^2} + \frac{1}{L_{\bar{b}c}^2} \tag{25}$$

Let us denote coordinate differences between points $\boldsymbol{b}$ and $\boldsymbol{a}$ as Δ_1 and Δ_2, see Fig. 13. We now substitute symbols A, B and C for the following distances

$$\begin{aligned}
L_{bc}^2 &= \Delta_{bc,1}^2 + \Delta_{bc,2}^2 = A \\
L_{\bar{b}c}^2 &= \left(\Delta_{bc,1} + \Delta_1\right)^2 + \Delta_{bc,2}^2 \\
&= A + \underbrace{2\Delta_{bc,1}\Delta_1 + \Delta_1^2}_{B} = A + B \\
L_{\bar{a}c}^2 &= \Delta_{bc,1}^2 + \left(\Delta_{bc,2} + \Delta_2\right)^2 \\
&= A + \underbrace{2\Delta_{bc,2}\Delta_2 + \Delta_2^2}_{C} = A + C \\
L_{ac}^2 &= \left(\Delta_{bc,1} + \Delta_1\right)^2 + \left(\Delta_{bc,2} + \Delta_2\right)^2 \\
&= A + B + C
\end{aligned} \tag{26}$$

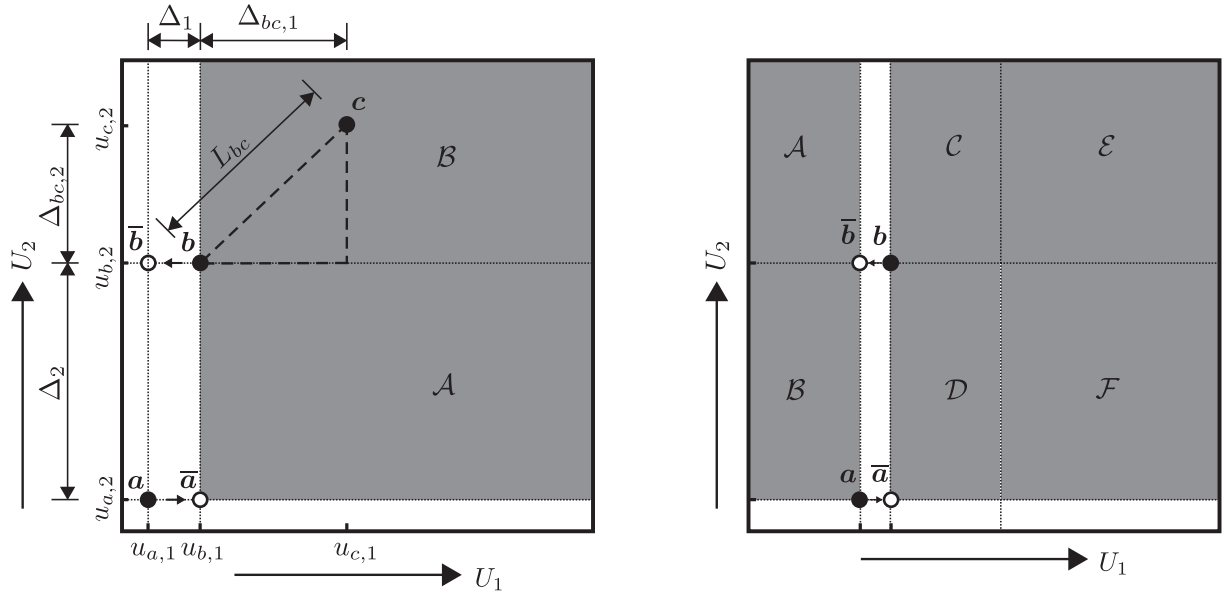

Fig. 13. On the non-uniformity of designs optimized using the original AE criterion.

Substituting these symbols into Eq. (25)

$$\frac{1}{A+B+C}+\frac{1}{A}>\frac{1}{A+C}+\frac{1}{A+B} \tag{27}$$

and rearranging this yields $(A+C)(A+B)>A(A+B+C)$ which, after expanding and subtracting identical terms on both sides, yields the final inequality $0<BC$. Since all deltas are positive, this is a valid statement and therefore Eq. (25) is also valid. We have proven that the optimization based on AE prefers to avoid corner points.

We can also show that not only corners but any point with some extreme coordinate U_i is attracted towards the center along the remaining coordinates. The proof for $N_{\text{var}}=2$ is almost the same, except we now consider six gray areas (Fig. 13 right). Switching $\boldsymbol{a}\to\bar{\boldsymbol{a}}$ and $\boldsymbol{b}\to\bar{\boldsymbol{b}}$ leads to the following changes in AE contributions (pairs within gray areas are omitted): $\boldsymbol{b}\mathcal{C}=\bar{\boldsymbol{b}}\mathcal{A}$, $\boldsymbol{b}\mathcal{A}=\bar{\boldsymbol{b}}\mathcal{C}$, $\boldsymbol{a}\mathcal{C}=\bar{\boldsymbol{a}}\mathcal{A}$, $\boldsymbol{a}\mathcal{A}=\bar{\boldsymbol{a}}\mathcal{C}$, $\boldsymbol{b}\mathcal{D}=\bar{\boldsymbol{b}}\mathcal{B}$, $\boldsymbol{b}\mathcal{B}=\bar{\boldsymbol{b}}\mathcal{D}$, $\boldsymbol{a}\mathcal{D}=\bar{\boldsymbol{a}}\mathcal{B}$, $\boldsymbol{a}\mathcal{B}=\bar{\boldsymbol{a}}\mathcal{D}$, $\boldsymbol{a}\mathcal{F}=\bar{\boldsymbol{b}}\mathcal{F}$, $\boldsymbol{b}\mathcal{F}=\bar{\boldsymbol{a}}\mathcal{F}$, however $\boldsymbol{a}\mathcal{E}+\boldsymbol{b}\mathcal{E}>\bar{\boldsymbol{a}}\mathcal{E}+\bar{\boldsymbol{b}}\mathcal{E}$. The last inequality term can be simply proven in exactly the same way as the proof concerning the corner point.

The proof is based on the assumption that when a given point is in the same distance from a center of a gray area, it also makes the same contribution to the AE criterion. This is of course not satisfied exactly; it is an expectation that should be approximately valid for a uniform design with a larger number of points in a gray area. A similar proof can also be obtained for other points, not only those with extreme coordinates. The assumption that AE design is uniform [1,3,17,18,21,24,28,58,59] is disproved.

Appendix B. Statistical moments Z_{exp}

Generally, in order to determine the mean value, standard deviation, skewness and excess kurtosis, one can use the kth central moments defined as

$$c_k=\int_{-\infty}^{\infty}\cdots\int_{-\infty}^{\infty}[g(\boldsymbol{x})-\mu]^k\,\mathrm{d}F_{\boldsymbol{X}}(\boldsymbol{x}) \tag{28}$$

In the case of function $g()$ defined in Eq. (22), the mean value μ (the first raw moment) equals

$$\mu_{\text{exp}}=N_{\text{var}}\frac{\sqrt{3}}{3}\approx 0.577\,350\,N_{\text{var}} \tag{29}$$

The central moments can be calculated analytically

$$\begin{aligned}
c_2 &= N_{\text{var}}\sqrt{5}/5-N_{\text{var}}/3\\
c_3 &= N_{\text{var}}\sqrt{7}/7-N_{\text{var}}\sqrt{15}/5+2N_{\text{var}}\sqrt{3}/9\\
c_4 &= \frac{14}{15}N_{\text{var}}(N_{\text{var}}-1)+\frac{2\sqrt{5}}{5}N_{\text{var}}(N_{\text{var}}-2)\\
&\quad-\frac{4}{21}N_{\text{var}}\sqrt{21}
\end{aligned} \tag{30}$$

Given these central moments, the standard deviation, skewness and excess kurtosis read

$$\begin{aligned}
\sigma_{\text{exp}} &= \sqrt{c_2}=\sqrt{N_{\text{var}}}\sqrt{\frac{\sqrt{5}}{5}-\frac{1}{3}}\\
&\approx 0.337\,461\sqrt{N_{\text{var}}}\\
\gamma_{\text{exp}} &= \frac{c_3}{c_2^{3/2}}=\frac{1}{21}\frac{15}{\sqrt{N_{\text{var}}}}\frac{\left(45\sqrt{7}-63\sqrt{15}+70\sqrt{3}\right)}{\left(3\sqrt{5}-5\right)^{3/2}}\\
&\approx -\frac{0.305\,281}{\sqrt{N_{\text{var}}}}
\end{aligned}$$

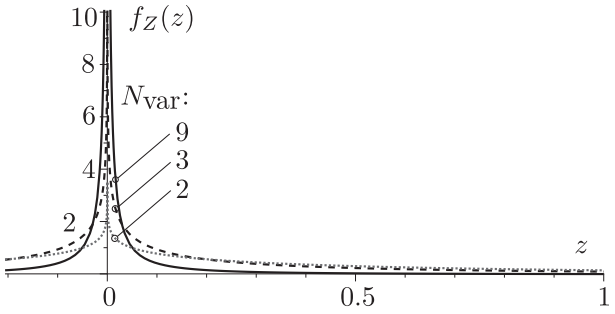

Fig. 14. Probability density function of a product of N_{var} independent standard Gaussian random variables. The function is symmetrical about zero.

$$\begin{aligned}
\kappa_{\text{exp}} &= \frac{c_4}{c_2^2}-3=\frac{30}{7}\cdot\frac{42\sqrt{5}-10\sqrt{21}-49}{N_{\text{var}}\left(3\sqrt{5}-5\right)^2}\\
&\approx -\frac{1.337\,875}{N_{\text{var}}}
\end{aligned} \tag{31}$$

The PDF of transformation g_{exp} slowly converges towards a Gaussian distribution. The PDF is visualized using insets in Fig. 10. It is nonzero in unit-length intervals from zero to N_{var} where it has N_{var} branches.

Appendix C. Probability density of Z_{prod}

The product of independent standard Gaussian random variables cannot be obtained in closed form, but it was derived in [52] using the Mellin transform to read

$$f_{\text{prod}}(z)=\frac{1}{(2\pi)^{N_{\text{var}}/2}}G^{N_{\text{var}},0}_{0,\,N_{\text{var}}}\left(\frac{z^2}{2^{N_{\text{var}}}}\,\middle|\,\underbrace{0,0,\ldots,0}_{N_{\text{var}}\text{ zeros}}\right) \tag{32}$$

where G is the Meijer G-function. In the case of two random variables ($N_{\text{var}}=2$), this density simplifies to $f_{\text{prod}}(z)=\frac{1}{\pi}K_0(|z|)$, where $K_0(\,\cdot\,)$ is the zeroth order modified Bessel function of the second kind. The PDF is visualized in Fig. 14. It can be seen that the distribution has relatively heavy tails, which renders the error produced by the AE method more pronounced.

Due to the symmetry of the PDF of variable $Z=Z_{\text{prod}}$, all odd raw moments equal zero; specifically the mean value $\mu_Z=0$ and also the skewness $\gamma_Z=0$. The even raw moments can be evaluated from the standard normal distribution by computing the absolute moments, since it is known that $E[|Z|^m]=\prod_{i=1}^{N_{\text{var}}}E[|X_\nu|^m]$, $m=0,1,2,\ldots$ The standard normal probability density reads $f_\nu(x_\nu)=\exp(-x_\nu^2/2)/\sqrt{(2\pi)}$ and therefore $E[|X_\nu|^m]=\int_{-\infty}^{\infty}|x_\nu|^m f_\nu(x_\nu)\,\mathrm{d}x_\nu$. The first two even raw moments of Z are: $E[Z^2]=1$ and $E[Z^4]=3^{N_{\text{var}}}$, for which the kurtosis of Z reads $\beta_Z=E[Z^4]/(E[Z^2])^2=3^{N_{\text{var}}}$ and the excess kurtosis of Z is $\kappa_Z=3^{N_{\text{var}}}-3$.

References

[1] Audze P, Eglājs V. New approach for planning out of experiments. Prob Dyn Strengths 1977;35:104–7. (in Russian)

[2] Auziņš J, Januševskis A, Januševskis J. Optimized experimental designs for metamodeling: algorithm. Scientif J RTU 6 series 2010;33:25–9.

[3] Bates SJ, Sienz J, Langley DS. Formulation of the Audze–Eglais uniform Latin Hypercube design of experiments. Adv Eng Softw 2003;34(8):493–506. doi:10.1016/S0965-9978(03)00042-5. ISSN 0965–9978.

[4] Bulik M, Liefvendahl M, Stocki R, Wauquiez C. Stochastic simulation for crashworthiness. Adv Eng Softw 2004;35(12):791–803. doi:10.1016/j.advengsoft.2004.07.002. ISSN 0965–9978.

[5] Conover WJ. On a better method for selecting input variables; 1975. Unpublished Los Alamos National Laboratories manuscript, reproduced as Appendix A of "Latin Hypercube Sampling and the Propagation of Uncertainty in Analyses of Complex Systems" by J.C. Helton and F.J. Davis, Sandia National Laboratories report SAND2001-0417.

[6] Elhewy AH, Mesbahi E, Pu Y. Reliability analysis of structures using neural network method. Probab Eng Mech 2006;21(1):44–53. doi:10.1016/j.probengmech.2005.07.002. ISSN 0266–8920.

[7] Fang K-T, Ma C-X. Wrap-around L_2-discrepancy of random sampling, latin hypercube and uniform designs. J Complex 2001;17(4):608–24. doi:10.1006/jcom.2001.0589. ISSN 0266–8920.

[8] Fang K-T, Wang Y. Number-theoretic methods in statistics. 1st ed. London ; New York: Chapman and Hall/CRC; 1993. ISBN 9780412465208.

[9] Fang K-T, Ma C-X, Winker P. Centered L_2-discrepancy of random sampling and latin hypercube design, and construction of uniform designs. Math Comput 2000;71(237):275–96. doi:10.1090/S0025-5718-00-01281-3. ISSN 1088–6842.

[10] Faure H, Lemieux C. Generalized Halton sequences in 2008: a comparative study. ACM Trans Model Comput Simul 2009;19(4) 15:1–15:31. doi: 10.1145/1596519.1596520.

[11] Fuerle F, Sienz J. Formulation of the Audze—Eglais uniform Latin hypercube design of experiments for constrained design spaces. Adv Eng Softw 2011;42(9):680–9. doi:10.1016/j.advengsoft.2011.05.004. ISSN 0965–9978.

[12] Fuerle F, Sienz J. Decomposed surrogate based optimization of carbon-fiber bicycle frames using optimum latin hypercubes for constrained design spaces. Comput Struct 2013;119:48–59. doi:10.1016/j.compstruc.2012.11.014.

[13] Goel T, Haftka RT, Shyy W, Watson LT. Pitfalls of using a single criterion for selecting experimental designs. Int J Numer Methods Eng 2008;75(2):127–55. doi:10.1002/nme.2242. ISSN 1097-0207.

[14] Halabi FE, González D, Chico-Roca A, Doblaré M. Multiparametric response surface construction by means of proper generalized decomposition: an extension of the PARAFAC procedure. Comput Methods Appl Mech Eng 2013;253:543–57. doi:10.1016/j.cma.2012.08.005.

[15] Halton JH. On the efficiency of certain quasi-random sequences of points in evaluating multi-dimensional integrals. Numerische Mathematik 1960;2(1):84–90. doi:10.1007/BF01386213. ISSN0029-599X.

[16] Hammersley JM, Handscomb DC. Monte Carlo methods. Taylor & Francis; 1964. ISBN 978-0416523409.

[17] Husslage BGM, Rennen G, van Dam ER, den Hertog D. Space-filling latin hypercube designs for computer experiments. CentER Discussion Paper. Tilburg University; 2008. 2008-104.

[18] Husslage BGM, Rennen G, van Dam ER, den Hertog D. Space-filling latin hypercube designs for computer experiments. Optim Eng 2011;12(4):611–30. doi:10.1007/s11081-010-9129-8. ISSN 1389–4420.

[19] Husslage BGM. Maximin designs for computer experiments. Tilburg University; 2006. Ph.D. thesis. 136 pages.

[20] Iman RC, Conover WJ. Small sample sensitivity analysis techniques for computer models with an application to risk assessment. Commun Stat-Theor Methods 1980;A9(17):1749–842.

[21] Janouchová E, Kučerová A. Competitive comparison of optimal designs of experiments for sampling-based sensitivity analysis. Comput Struct 2013;124(0):47–60. doi:10.1016/j.compstruc.2013.04.009. ISSN 0045–7949. Special Issue:.

[22] Johnson ME, Moore LM, Ylvisaker D. Minimax and maximin distance designs. Journal of Stat Planning Inference 1990;2(26):131–48. doi:10.1016/0378-3758(90)90122-B. ISSN 0378–3758.

[23] Khatir Z, Thompson H, Kapur N, Toropov V, Paton J. Multi-objective computational fluid dynamics (cfd) design optimisation in commercial bread-baking. Appl Thermal Eng 2013;60:480–6.

[24] Kovalovs A., Rucevskis S.. Identification of elastic properties of composite plate. In: Proceedings of annual conference on functional materials and nanotechnologies – FM&NT; vol. 23 of IOP Conf. Series: Materials Science and Engineering. IOP Publishing, Ltd; doi: 10.1088/1757-899X/23/1/012034.

[25] Kučerová A, Lepš M. Soft computing-based calibration of microplane M4 model parameters: methodology and validation. Adv Eng Softw 2014;72:226–35. doi:10.1016/j.advengsoft.2014.01.013. ISSN 0965–9978.

[26] Leary S, Bhaskar A, Keane A. Optimal orthogonal-array-based latin hypercubes. J Appl Stat 2003;30(5):585–98. doi:10.1080/0266476032000053691.

[27] Li G, Rosenthal C, Rabitz H. High dimensional model representations. J Phys Chem A 2001;105(33):7765–77. doi:10.1021/jp010450t. ISSN 1089–5639.

[28] Liefvendahl M, Stocki R. A study on algorithms for optimization of Latin hypercubes. J Stat Planning Inference 2006;136(9):3231–47. doi:10.1016/j.jspi.2005.01.007. ISSN 0378–3758.

[29] Mazars J. Application de la mécanique de l'endommagement au comportement non linéaire et à la rupture du béton de structure. Ph.D. thesis. Paris, France: Univ. Paris VI; 1984.

[30] McKay MD, Conover WJ, Beckman RJ. A comparison of three methods for selecting values of input variables in the analysis of output from a computer code. Technometrics 1979;21:239–45. doi:10.1080/00401706.1979.10489755.

[31] Morris MD, Mitchell TJ. Exploratory designs for computational experiments. J Stat Planning Inference 1995;43(3):381–402. doi:10.1016/0378-3758(94)00035-T. ISSN 0378–3758.

[32] Myers RH. Response surface methodology. Allyn and Bacon; 1971.

[33] Myšáková E, Lepš M, Kučerová A. A method for maximin constrained design of experiments. In: Topping B, editor. Proceedings of the eighth international conference on engineering computational technology. Civil-Comp Press, Stirlingshire, Scotland; 2012.

[34] Nasrellah HA, Manohar CS. A particle filtering approach for structural system identification in vehicle-structure interaction problems. J Sound Vibration 2010;329(9):1289–309. doi:10.1016/j.jsv.2009.10.041. ISSN 0022-460X.

[35] Nasrellah HA, Manohar CS. Finite element method based monte carlo filters for structural system identification. Probabilistic Engineering Mechanics 2011;26:294–307. doi:10.1016/j.probengmech.2010.08.006.

[36] Nelsen RB. An introduction to Copulas. Springer series in statistics, XIV. 2nd ed. Springer; 2006. ISBN 978-0-387-28659-4. Originally published as volume 139 in the series "Lecture Notes Statistics".

[37] Niederreiter H. Low-discrepancy and low-dispersion sequences. J Number Theor 1988;30(1):51–70. doi:10.1016/0022-314X(88)90025-X. ISSN 0022-314X.

[38] Novák D, Vořechovský M, Teplý B. FReET: Software for the statistical and reliability analysis of engineering problems and FReET-D: degradation module. Adv Eng Softw (Elsevier) 2014;72:179–92. doi:10.1016/j.advengsoft.2013.06.011. ISSN 0965–9978 Special Issue dedicated to Professor Zdeněk Bittnar on the occasion of his Seventieth Birthday: Part 2.

[39] Patzák B, Rypl D. Object-oriented, parallel finite element framework with dynamic load balancing. Adv Eng Softw 2012;47:35–50.

[40] Patzák B. OOFEM - an object-oriented simulation tool for advanced modeling of materials and structures. Acta Polytechnica 2012;52:59–66.

[41] Petelet M, Iooss B, Asserin O, Loredo A. Latin hypercube sampling with inequality constraints. AStA Adv Stat Anal 2010;94(4):325–39. doi:10.1007/s10182-010-0144-z. ISSN 1863–8171.

[42] Rabitz H, Ali merF. General foundations of high-dimensional model representations. J Math Chem 1999;25(2–3):197–233. doi:10.1023/A:1019188517934. ISSN 0259–9791.

[43] Rikards R, Chate A, Gailis G. Identification of elastic properties of laminates based on experiment design. Int J Solids Struct 2001;38(30–31):5097–115. doi:10.1016/S0020-7683(00)00349-8. ISSN 0020–7683.

[44] Robinson D, Atcitty C. Comparison of quasi- and pseudo-Monte Carlo sampling for reliability and uncertainty analysis. In: 40*th* AIAA structures, structural dynamics, and materials conference and exhibit. No. (AIAA-99-1589). In: AIAA/ASME/ASCE/AHS/ASC structures, structural dynamics and materials conference. St. Louis, MO, U.S.A.: American Institute of Aeronautics and Astronautics; 1999. p. 2942–9. doi:10.2514/6.1999-1589.

[45] Romero VJ, Burkardt JV, Gunzburger MD, Peterson JS. Comparison of pure and "Latinized" centroidal Voronoi tessellation against various other statistical sampling methods. Reliability Eng Syst Safety 2006;91(10–11):1266–80. doi:10.1016/j.ress.2005.11.023. ISSN 0951–8320, The Fourth International Conference on Sensitivity Analysis of Model Output (SAMO 2004).

[46] Rubenstein RY. Simulation and the Monte Carlo method. New York: John Wiley & Sons; 1981. New Press, Oxford.

[47] Sacks J, Schiller SB, Welch WJ. Designs for computer experiments. Technometrics 1989;31(1):41–7. doi:10.1080/00401706.1989.10488474.

[48] Shewry M, Wynn H. Maximum entropy design. J Appl Stat 1987;14(2):165–70. doi:10.1080/02664768700000020.

[49] Shields MD, Teferra K, Hapij A, Daddazio RP. Refined stratified sampling for efficient monte carlo based uncertainty quantification. Reliability Eng Syst Safety 2015;142:310–25. doi:10.1016/j.ress.2015.05.023. ISSN 0951–8320.

[50] Smith K. On the standard deviations of adjusted and interpolated values of an observed polynomial function and its constants and the guidance they give towards a proper choice of the distribution of observations. Biometrika 1918;12(1/2):1–85. ISSN 00063444.

[51] Sobol' IM. On the distribution of points in a cube and the approximate evaluation of integrals. USSR Comput Math Math Phys 1967;7(4):784–802. doi:10.1016/0041-5553(67)90144-9. ISSN 0041–5553.

[52] Springer MD, Thompson WE. The distribution of products of Beta, Gamma and Gaussian random variables. SIAM J Appl Math 1970;18(4):721–37. doi:10.1137/0118065.

[53] Tang B. Orthogonal array-based latin hypercubes. J Am Stat Assoc 1993;88(424):1392–7. doi:10.1080/01621459.1993.10476423.

[54] Vořechovský M. Optimal singular correlation matrices estimated when sample size is less than the number of random variables. Probab Eng Mech 2012;30:104–16. doi:10.1016/j.probengmech.2012.06.003. ISSN 0167–4730.

[55] Vořechovský M. Correlation control in small sample Monte Carlo type simulations II: analysis of estimation formulas, random correlation and perfect uncorrelatedness. Probab Eng Mech 2012;29:105–20. doi:10.1016/j.probengmech.2011.09.004. ISSN 0266–8920.

[56] Vořechovský M. Hierarchical refinement of latin hypercube samples. Comput-Aided Civil Infrastruct Eng 2015;30(5):394–411. doi:10.1111/mice.12088. ISSN 1467–8667.

[57] Vořechovský M, Novák D. Correlation control in small sample Monte Carlo type simulations I: A Simulated Annealing approach. Probab Eng Mech 2009;24(3):452–62. doi:10.1016/j.probengmech.2009.01.004. ISSN 0266–8920.

[58] Vu HM, Forth JP, Dao DV, Toropov VV. The use of optimisation for enhancing the development of a novel sustainable masonry unit. Appl Math Model 2014;38(3):853–63. doi:10.1016/j.apm.2013.07.026. ISSN 0307-904X.

[59] Bates SJ, Toropov VV, Querin OM. Generation of extended uniform latin hypercube designs of experiments. In: Topping B, editor. Proceedings of the ninth international conference on the application of artificial intelligence to civil, structural and environmental engineering. Civil-Comp Press, Stirlingshire, Scotland; 2007. p. 1–12.